The Canadian Mineralogist
Vol. 42, pp. 1541-1562 (2004)

THE ROLE OF SALINE FLUIDS BASE-METAL AND GOLD MINERALIZATION AT THE COBALT HILL PROSPECT NORTHEAST OF THE SUDBURY IGNEOUS COMPLEX, ONTARIO: A FLUID-INCLUSION AND MINERALOGICAL STUDY

EVA S. SCHANDL[§]

Department of Geology, University of Toronto, 22 Russell Street, Toronto, Ontario M5S 3B1, Canada

ABSTRACT

Pyrite-rich quartz veins that cut Huronian sediments at Cobalt Hill, Mackelcan Township, Ontario, *ca*. 20 km northeast of the Sudbury Igneous Complex (SIC), crystallized from saline hydrothermal fluids. The coarse-grained pyrite in the quartz veins contains minute inclusions of millerite, gersdorffite, pentlandite, chalcopyrite, chalcocite, pyrrhotite, coloradoite and gold, and primary fluid inclusions in the veins contain halite as a daughter mineral, and inclusions of pyrite, iron carbonate and micas. The primary fluid inclusions in the quartz veins have salinities of 26–46 equiv. wt% NaCl, an entrapment temperature close to 400°C, and pressure of *ca*. 1.3 kbar. The presence of chromian muscovite stringers in the quartz–pyrite veins suggests that the hydrothermal fluids were in contact with Cr-rich mafic or ultramafic rocks at some depth, whereas the variety of sulfide inclusions in pyrite suggests that the source rocks were enriched in base metals and possibly gold. The mobilization of base metals, Hg telluride and gold, and their subsequent precipitation in the quartz veins at Cobalt Hill, were facilitated by saline hydrothermal fluids that postdate the Sudbury Event. The fluids probably represent heated Canadian Shield brines mixed with hydrothermal fluids that crystallized the host quartz veins. The salinity and homogenization temperature of fluid inclusions in the veins are comparable to those of fluids that mobilized base-metal sulfides and possibly PGE in the South Range deposits, and base-metal sulfides in the North Range deposits of the SIC. The relative proximity of Cobalt Hill to the SIC, the ubiquitous presence of small Sudbury-type sulfide inclusions in pyrite in the Cobalt Hill quartz veins, the comparable salinity and homogenization temperature of fluid inclusions in these veins to those of metal-rich fluids of the SIC, and the presence of chromian muscovite, imply a spatial relationship of the veins to Sudbury-type base metals and to a Cr-rich mafic or ultramafic intrusion at depth.

Keywords: base metals, gold, saline fluids, fluid inclusions, Cobalt Hill prospect, Lake Wanapitei, Ontario.

SOMMAIRE

Les veines de quartz riches en pyrite qui recoupent les roches métasédimentaires d'âge huronien à Cobalt Hill, canton de Mackelcan, en Ontario, environ 20 km au nord-est du complexe igné de Sudbury, a cristallisé à partir de fluides hydrothermaux à salinité élevée. La pyrite à granulométrie grossière dans ces veines contient d'infimes inclusions de millerite, gersdorffite, pentlandite, chalcopyrite, chalcocite, pyrrhotite, coloradoïte et or, et des inclusions fluides primaires contenant la halite précipitée à partir du fluide piégé, et des inclusions accidentelles de pyrite, carbonate de fer et de micas. Les inclusions fluides primaires ont une salinité comprise entre 26 et 46% NaCl (ou équivalents, en poids), une température de piégeage voisine de 400°C, et une pression d'environ 1.3 kbar. La présence de muscovite chromifère en lambeaux dans les veines de quartz–pyrite fait penser que la phase fluide est entrée en contact avec des roches mafiques ou ultramafiques riches en Cr à profondeur. Aussi, la variété d'inclusions de sulfures dans la pyrite indique que les roches à la source étaient enrichies en métaux de base, et peut-être en or. La mobilisation des métaux de base, du tellurure de mercure, et de l'or, et leur précipitation par la suite dans des veines de quartz, ont été facilitées par les fluides hydrothermaux à salinité élevée postérieurs à l'événement d'impact à Sudbury. Ces fluides représenteraient des saumures chauffées du Bouclier Canadien mélangées aux fluides desquels ont cristallisé les veines de quartz. Leur salinité et les températures de leur homogénéisation sont comparables à celles des fluides qui ont mobilisé les sulfures de métaux de base et les éléments du groupe du platine dans les gisements du flanc sud, et les métaux de base du flanc nord, du complexe de Sudbury. La proximité de Cobalt Hill à ce complexe, la présence ubiquiste de petites inclusions de sulfures de type Sudbury dans la pyrite des veines de quartz à Cobalt Hill, la salinité et les températures d'homogénéisation comparables des inclusions fluides à celles du complexe de Sudbury, et la présence de muscovite chromifère supposent une relation spatiale des veines aux accumulations de métaux de base de type Sudbury et à des roches mafiques ou ultramafiques chromifères à profondeur.
(Traduit par la Rédaction)

Mots-clés: métaux de base, or, fluides à salinité élevée, inclusions fluides, indice de Cobalt Hill, Lac Wanapitei, Ontario.

§ *E-mail address*: eschandl@consultgeo.com

Introduction

In the present study, I combine fluid-inclusion systematics with mineralogy to investigate the nature of hydrothermal fluids that gave rise to pyrite-rich quartz veins containing small inclusions of millerite, pentlandite, pyrrhotite, chalcopyrite, chalcocite, coloradoite and gold at the Cobalt Hill base-metal – gold prospect, *ca.* 20 km northeast of the Sudbury Igneous Complex (SIC), Ontario. Because numerous base-metal and precious-metal prospects are known in the area, a better understanding of the source and origin of metal-bearing fluids at Cobalt Hill could provide important information for exploration east of the SIC.

Huronian sedimentary rocks are locally enriched in base and precious metals east of the SIC and Lake Wanapitei. The origin of these metals is enigmatic and has been a topic of debate over the last few decades (*cf.* Innes & Colvine 1979, 1984, Dressler 1982, Rowell & Edgar 1986, Gates 1991). Owing to the complex tectonic and metamorphic evolution of the area, the source of the metals and the mechanisms responsible for their mobilization and concentration are difficult to identify. As high concentrations of metals are commonly associated with shear zones and faults, and most mineralized zones are located within brecciated and hydrothermally altered sediments or sheared gabbroic rocks (*cf.* Gates 1991, Rowell & Edgar 1986), metamorphism is considered by these authors to have played an important part in their mobilization, redistribution and concentration.

My objectives here are: 1) to characterize the fluids instrumental in the mobilization of base metals and gold at Cobalt Hill, which represents one of several base-metal and gold prospects east of the SIC, 2) to compare the chemical composition and temperature of fluids that precipitated the quartz–pyrite veins at Cobalt Hill with fluids reported from the ore zone of the SIC, 3) to suggest a possible source for the metals, and 4) to identify the metamorphic event that may have been instrumental in the mobilization and concentration of metals.

Geological Setting

Cobalt Hill is located on the northeastern margin of Lake Wanapitei in Mackelcan Township, Ontario, *ca.* 20 km northeast of the SIC (Fig. 1). The area straddles the western margin of the Wanapitei magnetic and gravity high anomaly. Situated approximately 200 m north of Jones Lake and 200 m east of Jess Lake, Cobalt Hill is contained within an intensely microbrecciated and hydrothermally altered zone, *ca.* 100 m in diameter. This small area is part of a northwest-trending, intermittently

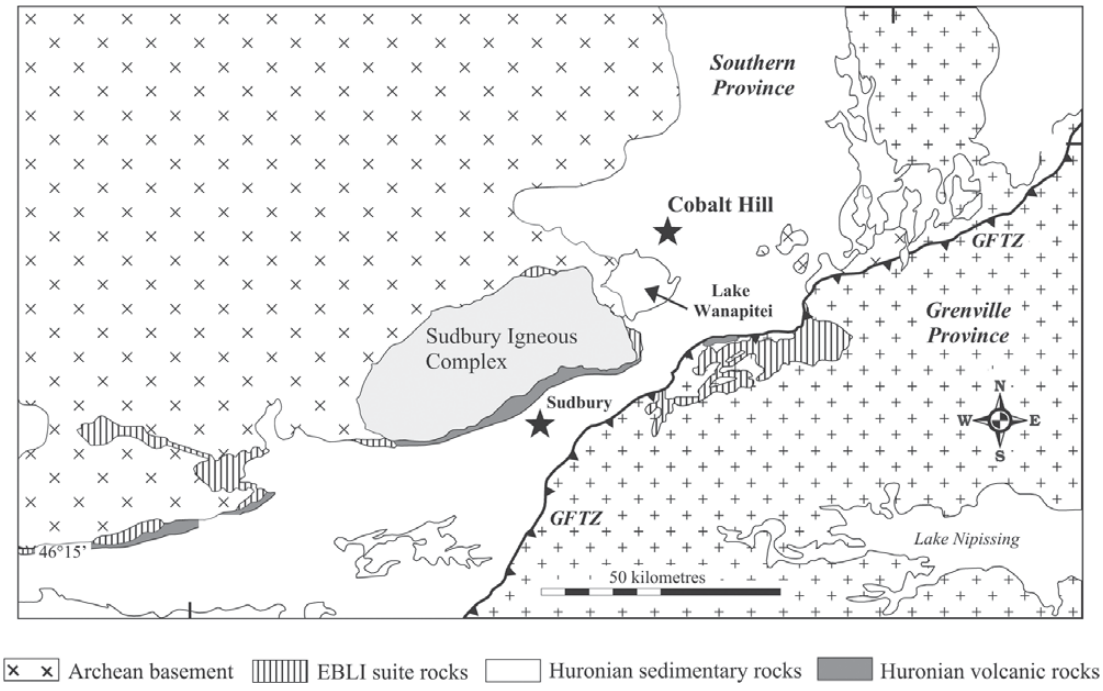

FIG. 1. Regional map of Cobalt Hill and the Sudbury Igneous Complex (from Peck *et al.* 2001).

albitized breccia zone 450 m long and 600 m wide that also contains the Jess Lake gold prospect. Gold values up to 7.5 grams per tonne have been reported from grab samples at Cobalt Hill, and up to 22.7 grams per tonne (in a 1.5-m-long drill-core section) from the Jess Lake gold prospect 60 m west of Cobalt Hill (Flag Resources Ltd., company reports). Gold mineralization at Cobalt Hill is coupled with anomalous Ni (0.34%), Co (0.55%) and Cu (0.09%) values (Goad 1991).

The property contains exposures of Huronian sedimentary rocks of the Cobalt Group, which represents the uppermost sedimentary cycle of the Huronian Supergroup. The sedimentary units consist predominantly of quartz arenites mixed with minor arkosic quartzites of the Lorrain Formation. The age of the Huronian Supergroup is bracketed between that of the Copper Cliff rhyolites at the base of the Supergroup and the Murray Granite, at 2.45 and 2.47 Ga, respectively (Krogh *et al*. 1984, 1996), and the Nipissing gabbro that was emplaced in the Huronian sedimentary rocks at 2.22 Ga (Noble & Lightfoot 1992).

The Lorrain quartzites at Cobalt Hill are extensively brecciated and are cut by numerous quartz veins (up to 3 m wide) that contain and are converted to assemblages with albite, mica and chlorite. Metamorphic grade in the area is in the lower greenschist facies. Partial alteration of the sedimentary rocks to albite is widespread on a regional scale, extending for hundreds of kilometers; the western limit has been traced to the Bruce mines, and the eastern limit to Lake Temagami (Gates 1991). The age of albitization has been determined from the U–Pb age of Th-poor hydrothermal monazite in the nearby Scadding and MacLennan townships at 1.7 Ga (Schandl *et al*. 1992, 1994), indicating that this regional hydrothermal episode postdated the Sudbury Event of 1.85 Ga (Krogh *et al*. 1984). The 1.7 Ga monazite age corresponds to a period of granitic plutonism in the Southern Province, the time of collisional orogeny and the development of the Killarney Magmatic Belt (Easton 2000).

A map of the area that contains Cobalt Hill is shown in Figure 2. Samples collected for the fluid inclusion and mineralogical study include drill-core sections taken at 640 m depth from the deepest hole (759 m) drilled on Cobalt Hill (CH92–1), from outcrops adjacent to the drill hole and from the main waste pile. DDH92–1 represents one of the twelve drill holes put down at Cobalt Hill. A schematic cross-section of the drill-hole log for DDH92–1 is shown in Figure 3.

Previous Work

Highly saline fluids have been reported in fluid inclusions from ore zones along the North and South ranges of the SIC by Farrow & Watkinson (1992), Farrow *et al*. (1994), Li & Naldrett (1993), and Molnar *et al*. (1997, 1999, 2001). In their detailed work on fluid inclusions, these authors characterized the chemical properties and temperature of the hydrothermal fluids involved in the mobilization and deposition of some metals in deposits of the North and South ranges. They suggested a magmatic origin for the ore-bearing saline fluids. Temperatures of homogenization (T_h halite) of primary fluid inclusions from the Strathcona Deep Copper Zone, from Barnet, and from the Fraser Epidote zone define a range of 180°–250°C (Farrow & Watkinson 1992). In sulfide and precious metal-rich veins at the Little Stobie deposits, the primary fluid inclusions have a total T_h range of 180°–270°C (orebody 1) and 280°–350°C (orebody 2) (Molnar *et al*. 1999). Most primary fluid inclusions contain halite and a variety of other daughter minerals, and the salinity of the fluid ranges from 30 to 50 equiv. wt% NaCl or NaCl–$CaCl_2$ (Farrow & Watkinson 1992, Farrow *et al*. 1994, Li & Naldrett 1993, Molnar *et al*. 1997, 1999). Molnar *et al.* (2001) demonstrated the involvement of high-temperature fluids ($T_{h\ (total)}$ 400–500°C) released from a granophyre in the genesis of the vein-type Cu–Ni–PGE ores in the North Range. Molnar *et al.* (1999, 2001) distinguished between saline magmatic fluids and heated Canadian Shield brines in the Sudbury ore zones on the basis of their metal content, and suggested that the presence of saline fluid inclusions with a high content of metals could be used an exploration guide for vein-type Cu–Ni–PGE ores within the footwall of the Sudbury Structure.

The presence of high-salinity fluid inclusions at the SIC is not surprising, as in earlier studies of basement fluids, Fritz & Frape (1982) reported the presence of saline brines in the Sudbury area. In fact, the occurrence of saline waters and brines has been known for several decades within the Canadian Shield, and their geochemical and isotopic characteristics have been documented in detail (Fritz & Frape 1982, Frape & Fritz 1987). The brines were encountered at depths exceeding 1 km, and generally occur in shear zones or in pockets, under high pressure (Fritz & Frape 1982). Although most saline brines described by these authors were collected from operating mines, saline brines also have been identified in granitic plutons in the area at 1 km depth (Leech & Pearson 1981). The origin of the Shield brines is controversial, and hypotheses suggested for their origin include 1) modified seawater or basinal brines (Kelly *et al*. 1986, Guha & Kanwar 1987), 2) removal of saline fluids from fluid inclusions in crystalline rocks during episodes of high water–rock interaction (*cf*. Frape & Fritz 1987, Kamineni 1987), and 3) equilibrium reactions between low-temperature fluids and aluminosilicates (Kyser & Kerrich 1990). Kyser & Kerrich demonstrated with activity diagrams that the composition of the Shield fluids are controlled by kaolinite, muscovite and, to a lesser degree, feldspars, and thus, are distinct from seawater and brines. The isotopic composition of the Shield brines in the Sudbury area is unusual, as they have high δD values and plot to the left of the standard meteoric water line (SMWL) (Fritz & Frape 1982). Kyser & Kerrich (1990) suggested that the

high δD value of these brines is most likely the result of preferential loss of H^+ to low-δD methane (–500 to –100‰) that coexists with the brines (Fritz *et al.* 1987) and proposed that the low-δD methane acted as a sink for the hydrogen. High-δD fluids were recently reported from the epidote-altered vein-type ores in the footwall of the SIC by Marshall *et al.* (1999). On the basis of results from their fluid inclusion and isotope study, Marshall *et al.* suggested that the high values of δD can be attributed to fluid mixing between magmatic fluids and Sudbury-type groundwater.

Analytical Techniques

All analyses were carried out at the Department of Geology, University of Toronto. Microthermometric measurements on fluid inclusions were obtained on a Linkam THMS 600 fluid inclusion stage at the F. Gordon Smith Fluid Inclusion Laboratory, following the guidelines of Macdonald & Spooner (1981).

Daughter minerals were analyzed in open fluid-inclusion cavities (qualitative) with a JEOL 840 SEM equipped with energy-dispersion spectrometers (EDS). Quartz surfaces that contained the fluid inclusions were broken prior to placing the chips into the SEM, and daughter minerals and some accidental inclusions in the cavities were analyzed (qualitative) to identify the elements present. Operating conditions were: 15 kV, beam current 1 nA, take-off angle 40°, counting time 80 s.

Selected minerals were analyzed with an ETEC electron microprobe equipped with an EDS detector (operating conditions: 20 kV, 100 nA), using the following

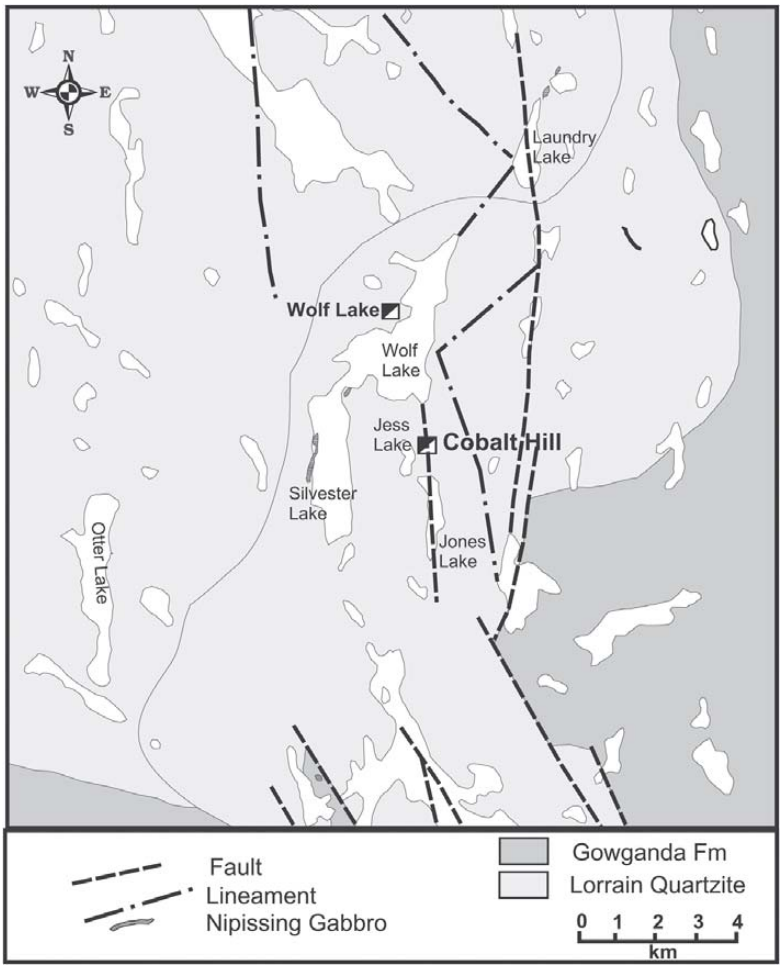

FIG. 2. Location map of Cobalt Hill (after Allen 2003).

standards: NIST for Au, REE standards (LaF_3, CeF_3, PrF_3, NdF_3) and pure metals for monazite, and natural mineral standards for all other minerals.

Mineralogy and Texture

The Lorrain quartzites at Cobalt Hill consist of angular to subrounded quartz ± albite, variable proportions of minor muscovite, carbonate and chlorite. The rocks are albitized, brecciated, and silicified, with several generations of quartz veins. Some of the early veins are fractured, fragmented and brecciated, and fractures are filled by muscovite, locally chromian, radiating chlorite, carbonate and quartz. Aggregates of pyrite and disseminated pyrite locally form sulfide-rich domains in the early quartz veins, and their textural relationship to quartz suggests contemporaneous crystallization. The estimated content of pyrite through a 750-m drill-core section (DDH 92–1) is *ca.* 3–5%, but pyrite locally occurs in massive, up to 50 cm wide bands within the drill core (Goad 1992). Fragmented pyrite contains an abundance of minute inclusions of Ni–Cu sulfide, pyrrhotite, some mercury telluride (coloradoite) and gold (Schandl 2002).

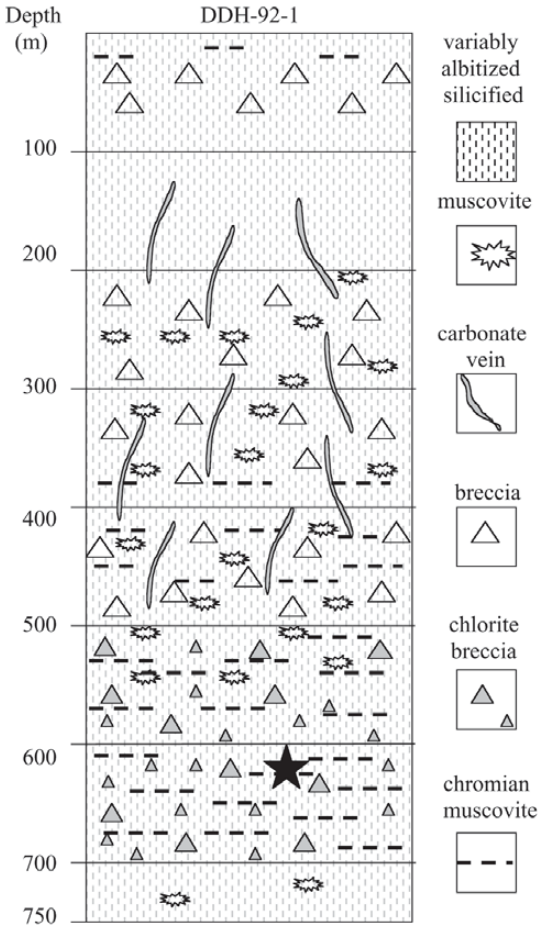

FIG. 3. Schematic cross-section of drill hole DDH92–1. Star represents the location of the core samples used in this study.

Detailed log descriptions of hole DDH 92–1 by Goad (1992) make it possible to identify the major types of alteration, the distribution of breccia zones and the sulfides within the 750-m section of Lorrain quartzites. The section contains two distinct breccia zones, upper and lower zone, and the common replacement minerals include albite, quartz, chlorite white micas, chromian muscovite and carbonate. Two types of breccia were identified, type 1 and 2. Type-1 breccia includes the uppermost breccia–microbreccia zone at *ca.* 129 m depth, and the upper part of the lower breccia zone at *ca.* 475 m. It consists of hematite-coated (salmon pink to red) fragments of albitized quartzite healed by small quartz and minor chlorite veinlets. The type-2 breccia occurs within the lower breccia zone at 500–685 m depth, and consists of fragments of albitized quartzite up to 15 cm in diameter, with abundant interstitial chlorite and an abundance of quartz veins that cut the quartzite. Stacks of chromian mica (locally up to 5–10%) are included in the quartz veins. Silicification is apparent throughout the entire 750-m core; the addition of quartz is manifest in siliceous "marbling" of the albitized quartzite and in the abundance of quartz veins.

The mineralogy and texture of the hydrothermally altered rocks at Cobalt Hill are described below, and mineral assemblages in selected samples are listed in Appendix 1.

Quartz

Quartz represents the most significant secondary mineral at Cobalt Hill. The addition of SiO_2 to the orthoquartzite in the form of quartz veins and quartz pods implies large-scale hydrothermal activity in the area. At least two generations of quartz veins are distinguished. The earlier quartz occurs as coarse-grained veins, some of which are fractured and fragmented, and the fractures were filled either by second-generation quartz, fine-grained muscovite, chromian muscovite, chlorite or carbonate. Second-generation quartz is volumetrically less important, the small veins filling fractures in earlier quartz veins and occurring as a late overgrowth on earlier coarse-grained quartz and on pyrite. Pyrite containing inclusions of Ni–Cu sulfides, gold and coloradoite is associated with the earlier quartz veins and quartz pods. Some veins are vuggy, plumose quartz is common in the veins, and small, euhedral quartz with growth bands (Figs. 4a–c) is interstitial to the plumose quartz. Most quartz in the veins is exten-

sively strained and has undulose extinction. Some quartz is iron-stained, and the parallel alignment of minute flakes of hematite (?) in quartz suggests that they fill microfractures. Although fluid inclusions are abundant in most quartz, they are absent in the Fe-stained grains.

Muscovite and chromian muscovite

Muscovite aggregates occur as contorted veinlets in fractured quartz, and as inclusions in quartz (Fig. 4d), but they are relatively rare in the quartzite. Muscovite and coexisting chromian muscovite occur in radiating aggregates interstitial to quartz and as rims on pyrite. Because most mica is associated with fractured, first-generation quartz veins, fractured pyrite and brecciated sediments, it appears to represent a later stage (or the waning stage) in the hydrothermal evolution of the rocks. Results of electron-microprobe analyses of selected muscovite domains are presented in Table 1. Some muscovite contain 1.5–2.5 wt % Cr_2O_3 and up to 0.49 wt% vanadium (V_2O_5); both Cr and V substitute for ^{VI}Al, and signal an influx from a probable external mafic or ultramafic source.

Carbonate

Carbonate veins fill fractures in the first-generation quartz veins and occur as fine-grained aggregates within the sedimentary rocks. Most carbonate aggregates are fine-grained and Fe-stained and range in compositions from calcite to ferroan dolomite and ankerite. Aggregates of fine-grained carbonate grains are interstitial to radiating sheafs of muscovite, but some carbonate grains are rimmed by mica flakes. Textural relationships between the carbonates and mica suggest that crystallization was more or less contemporaneous. Some of the veinlets of second-generation quartz contain aggregates of calcite, suggesting that the crystallization of carbonates occurred throughout the hydrothermal evolution of the rocks.

The feldspars

The feldspar grains define a narrow range in composition from almost pure albite to oligoclase (An_{5-15}). The feldspar occurs as detrital grains in the quartzite and as replacement of detrital quartz and K-feldspar. Secondary albite is identified by its typical "chessboard" texture characteristic of albitized rocks in the region (*cf.* Schandl *et al.* 1994). Most feldspar grains (detrital and replacement) are iron-stained and contain minute globules of hematite (?) and iron oxyhydroxide.

Chlorite

Chlorite occurs on slip surfaces, in highly brecciated quartz veins, and in the brecciated quartzite. The chlorite content of the rock attains 25%, particularly where it is a matrix to the brecciated quartzite (Flag Resources internal reports). Most aggregates of chlorite are interstitial to quartz in the veins and to the albitized quartzites. The composition of the vein-filling, fan-shaped chlorite, a clinochlore, is shown in Table 1. As the chemical composition of chlorite and variations in site occupancy (^{IV}Al) are temperature-dependent (Cathe-

TABLE 1. COMPOSITION OF SELECTED MINERALS FROM THE COBALT HILL PROSPECT, ONTARIO

Sample	CH-7C	CH-7C	CH-7B	CH-7B	CH-7B	CH-7B	CH-7B	CH-7C	CH-7C
Mineral	Pn	Pn	Mlr	Mlr	Gdf	Gdf	Brv ?	Cp	Po
Ni wt%	41.33	41.51	58.86	62.13	35.53	38.73	39.46		
Fe	26.33	25.75	4.97	2.86	3.03	3.45	4.40	31.67	60.30
Cu								33.35	
As					33.68	23.93	17.48		
Co									
S	33.03	32.85	36.22	35.80	28.50	34.19	41.37	34.61	38.90
Total	100.69	100.11	100.05	100.79	100.74	100.30	102.71	99.63	99.20

Sample	CH-3B	CH-3B	Sample #	CH-7C	CH-7C	CH-7C	CH-7C
Mineral	Mnz ^	Mnz ^		Clr	Clr	Au	Au
La_2O_3	16.12	11.74	Au			99.38	99.76
Ce_2O_3	32.29	31.37	Ag				
Nd_2O_3	6.51	10.82	Te	38.76	38.96		
Sm_2O_3	3.83	4.59	Hg	61.13	60.64		
ThO_2							
P_2O_5	31.20	31.23					
Total	89.95	89.75	Total	99.89	99.60	99.38	99.76

Sample #	CH-7B	CH-7B	CH-4A	CH-4A	CH-4A	CH-4A	CH-4B
Mineral	Ms	Ms	Ms	gr Ms	gr Ms	gr Ms	Chl
SiO_2 wt%	46.23	46.81	46.16	46.81	46.74	46.94	27.53
TiO_2			0.38				
Al_2O_3	35.36	34.30	33.80	37.99	32.52	37.81	19.71
Cr_2O_3				1.39	2.08	1.10	
V_2O_5				0.27	0.29	0.26	
FeO*	1.05	1.65	1.39	0.54	1.53	0.39	15.35
MgO	4.30	3.90	3.90		1.52		27.18
K_2O	10.29	10.10	10.18	8.11	10.18	7.77	
Na_2O	1.55	1.00	0.81				
Total	98.78	97.76	96.62	95.11	94.86	94.27	89.77
Si *apfu*	5.971	6.099	6.084	6.112	6.271	6.156	5.381
^{IV}Al	2.029	1.901	1.916	1.888	1.729		2.619
^{VI}Al	3.355	3.366	3.335	3.957	3.415	5.844	1.921
Cr				0.143	0.221	0.114	
Ti			0.037				
V				0.023	0.025	0.024	
Fe	0.113	0.180	0.153	0.058	0.172	0.043	2.508
Mg	0.827	0.757	0.766				7.918
Na	0.388	0.253	0.207				
K	1.696	1.678	1.711	1.300	1.365	1.300	

Note: blank: not detected, FeO* = total Fe. Mineral symbols: Pn pentlandite, Mlr millerite, Gdf gersdorffite, Brv bravoite, Cp chalcopyrite, Po pyrrhotite, Mnz monazite, Clr coloradoite, Au gold, Ms muscovite, gr Ms green muscovite, Chl chlorite. Mnz ^: results of semiquantitative analyses. For muscovite, the structural formula is calculated on the basis of 22 atoms of oxygen; for chlorite (clinochlore), 28 atoms of oxygen.

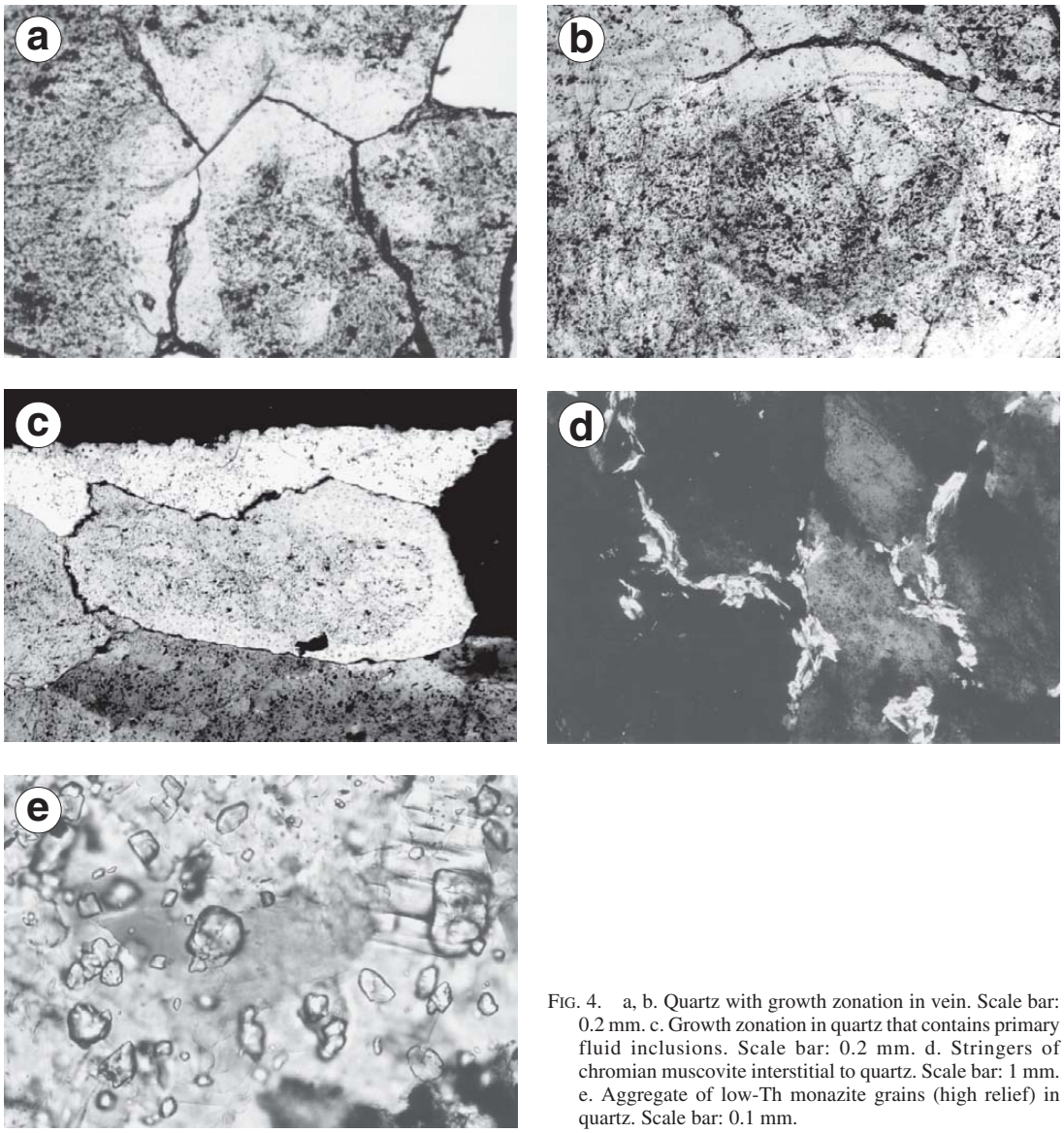

FIG. 4. a, b. Quartz with growth zonation in vein. Scale bar: 0.2 mm. c. Growth zonation in quartz that contains primary fluid inclusions. Scale bar: 0.2 mm. d. Stringers of chromian muscovite interstitial to quartz. Scale bar: 1 mm. e. Aggregate of low-Th monazite grains (high relief) in quartz. Scale bar: 0.1 mm.

lineau & Nieva 1985), chlorite can be used as a geothermometer. Thus, using the equation of Cathelineau & Nieva (1985), together with the (Fe) correction of Kranidiotis & MacLean (1987), the temperature of crystallization of chlorite in the first-generation quartz vein (CH–4B) is calculated to be 316 ± 25°C.

Monazite-(Ce)

Fine-grained, Th-poor monazite is an important accessory mineral in the quartzites and in the quartz veins (Table 1). A hydrothermal origin for the monazite is suggested by the lack of detectable Th in it (Schandl *et al.* 1994, Schandl & Gorton 2004). Monazite aggregates occur as inclusions in vein quartz within the first-generation veins at Cobalt Hill (Fig. 4e), as stringers in muscovite veinlets, and interstitial to the albitized quartzites. Monazite grains, having similar morphology and geochemistry, have been identified (and dated by U–Pb) in hydrothermally altered quartzites at the nearby Scadding gold mine and at the Sheppard gold occurrence (*ca.* 20 km south of Cobalt Hill), where they are

considered to have crystallized during the episode of sodium metasomatism (albitization) of the host sedimentary rocks at 1.7 Ga (Schandl *et al.* 1992, 1994). Th-poor monazite is known to occur in hydrothermal ore deposits worldwide, where it crystallizes from hydrothermal fluids (*cf* Schandl & Gorton 1991, Schandl *et al.* 1994, Compston & Matthai 1994, Wang *et al.* 1994, Schandl & Gorton 1994). Because albite at Cobalt Hill predated, or was more or less contemporaneous with, the pyrite-rich quartz veins, the time of vein emplacement (and the crystallization of pyrite, Ni–Cu sulfides and gold) may be constrained by the presence of Th-poor hydrothermal monazite in the muscovite-, carbonate-, and chlorite-bearing quartz veins. Their age is probably comparable to the 1. 7 Ga age of formation of the hydrothermal monazite at the Scadding gold mine and the Sheppard gold occurrence.

Sulfides

Subhedral to euhedral grains of pyrite occur as coarse-grained aggregates within first-generation vein quartz, some of which are fragmented and brecciated, as well as poikiloblasts that overgrow the sediment fabric. Some of the pyrite grains are fractured and fragmented, and pyrite is rimmed by fine-grained muscovite, chlorite and carbonate. Textural relationships between pyrite and vein quartz suggest that the crystallization of pyrite was predominantly contemporaneous with the first-generation veins, and that pyrite poikiloblasts in the host rocks are metamorphic, and not detrital in origin. Some pyrite does, however, occur in late quartz veinlets, or as small poikiloblasts that overgrow the earlier coarse-grained vein quartz.

Minute (30–500 μm) inclusions of Ni–Cu sulfides (pentlandite, millerite, gersdorffite, chalcopyrite and chalcocite) are present in pyrite (Figs. 5a–h) of the first-generation quartz veins. It is emphasized that sulfide inclusions are never associated with fractures within the pyrite, nor are they present in the late poikiloblasts of pyrite. Other small inclusions in the first-generation pyrite include pyrrhotite, coloradoite, gold, and a Ni-rich sulfide having a composition intermediate between gersdorffite and bravoite. All of the inclusions in pyrite were identified by their optical properties and chemical composition (Table 1).

The Ni concentration of pentlandite is relatively high at 41 wt%, and the As content in gersdorffite fluctuates between 33 and 24 wt%. The high Ni content of pentlandite is consistent with observations by Misra & Fleet (1973) and Craig & Scott (1982), that pentlandite has its highest Ni concentration where coexisting with millerite and pyrite. All sulfide inclusions in pyrite are anhedral; some are teardrop-shaped, some are subrounded, skeletal, elongate, and worm-shaped. Chalcocite is relatively common, occurring as replacement of chalcopyrite. Gold occurs as minute inclusions in pyrite, and some are intergrown with coloradoite (Fig. 5h). Results of electron-microprobe analyses of selected sulfides, gold and coloradoite are shown in Table 1. It should be noted that the Ni–Cu sulfides, coloradoite and gold are present only in the pyrite-rich quartz veins, and that none were identified in the quartzitic host-rocks.

The small inclusions of Ni–Cu sulfides, gold and coloradoite in pyrite within first-generation vein quartz at the Cobalt Hill prospect bear a striking similarity to the sulfide assemblages in some hydrothermal veins of the SIC (*cf.* Molnar *et al.* 1999).

Petrography of the Fluid Inclusions

Fluid inclusions were identified in first-generation quartz veins and in coarse-grained quartz-rich pods. Although the quartz veins at Cobalt Hill are composite, consisting of more than one generation, only the major, first-generation veins, believed to have been contemporaneous with sulfides and gold, were included in this investigation. Three types of fluid inclusions were identified in the quartz veins: type I: saturated aqueous fluid inclusions that consist of H_2O liquid, a vapor bubble, and one or more of daughter minerals (halite, mostly) ± accidental inclusions (Fig. 6a); type II: aqueous fluid inclusions that consist of liquid and vapor H_2O, and type III: CO_2-rich fluid inclusions that consist of CO_2 vapor + liquid and H_2O liquid (Fig. 6b). Type-I inclusions are the most abundant, and type-III are the least abundant. Most fluid inclusions are irregularly shaped, particularly those that contain daughter minerals. The size of halite crystals varies in type-I inclusions, making up 10 to 90% of the individual fluid inclusions (Fig. 6c), and the degree of fill for the two-phase fluid inclusions ranges from 50 to 90%. None of the CO_2-rich inclusions contains daughter minerals or accidental inclusions.

Primary and secondary fluid-inclusions were identified in the sulfide-rich vein quartz, and in the quartz-rich pods contemporaneous with the veins. Primary inclusions range in size from 3 to 25 μm, they occur in growth bands (Fig. 4c), and in distinct clusters within

FIG. 5. Coarse-grained pyrite with minute inclusions of Cu–Ni sulfides, coloradoite and gold. a. Inclusions of pentlandite (pn), chalcopyrite (cp) and chalcocite (cc) in pyrite. Scale bar: 0.2 mm. b. Inclusions of pentlandite (pn) and chalcopyrite (cp) in pyrite. Scale bar: 0.2 mm. c. Chalcocite (cc) inclusion in pyrite. Scale bar: 1 mm. d. Pentlandite (pn) and chalcopyrite (cp) inclusions in pyrite. Scale bar: 0.2 mm. e. Chalcocite (cc) and chalcopyrite (cp) inclusions in pyrite. Scale bar: 0.2 mm. f. Numerous small inclusions of chalcocite in pyrite. Scale bar: 0.2 mm. g. Numerous small inclusions of chalcocite and pentlandite in pyrite. Scale bar: 0.2 mm. h. Gold (Au), coloradoite (Clr) and chalcopyrite (cp) inclusions in pyrite. Scale bar: 0.1 mm.

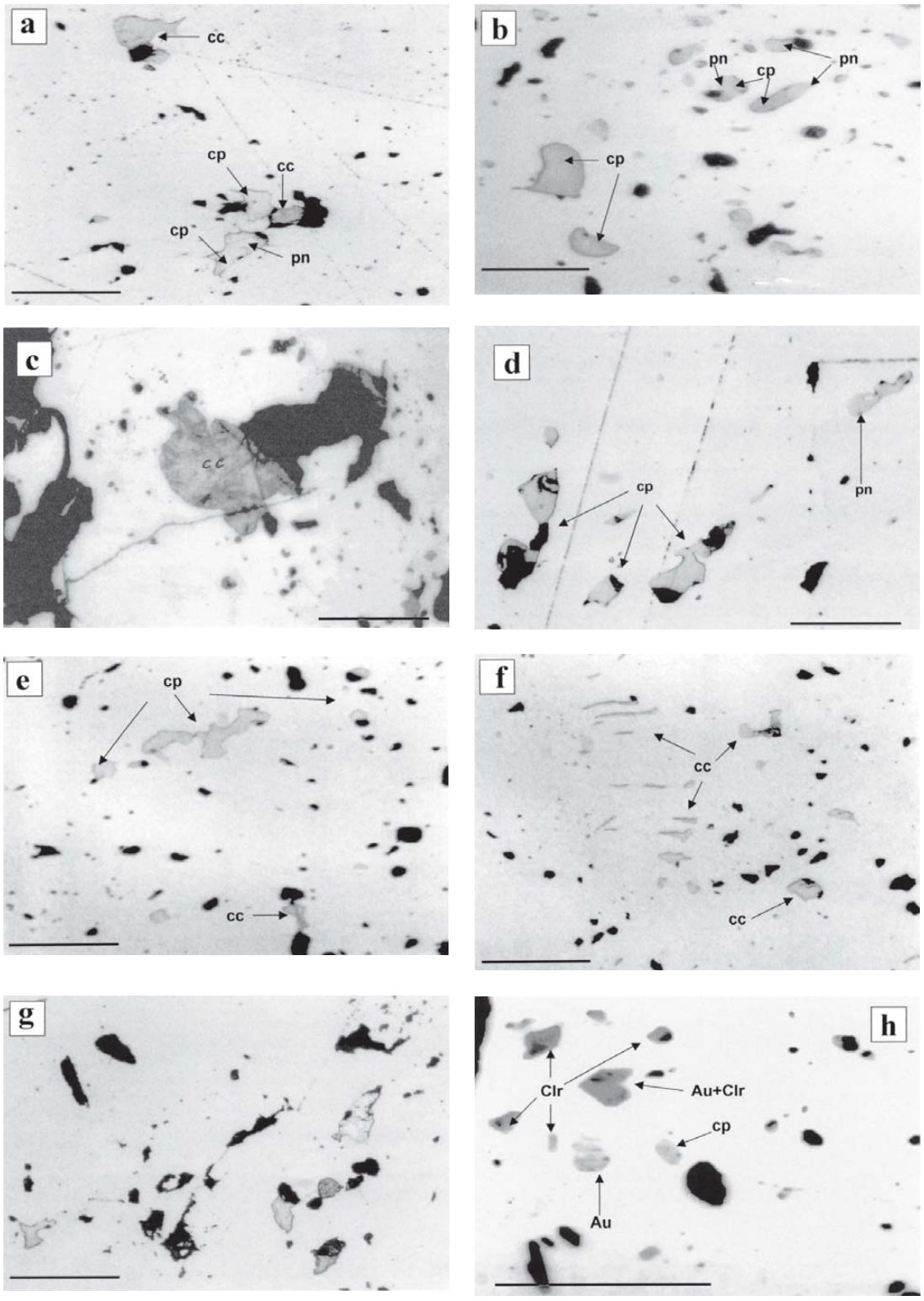
a
cc
cp
cc
cp
pn
b
pn
cp
pn
cp
c
cc
d
cp
pn
e
cp
cc
f
cc
cc
g
h
Clr
Au+Clr
cp
Au

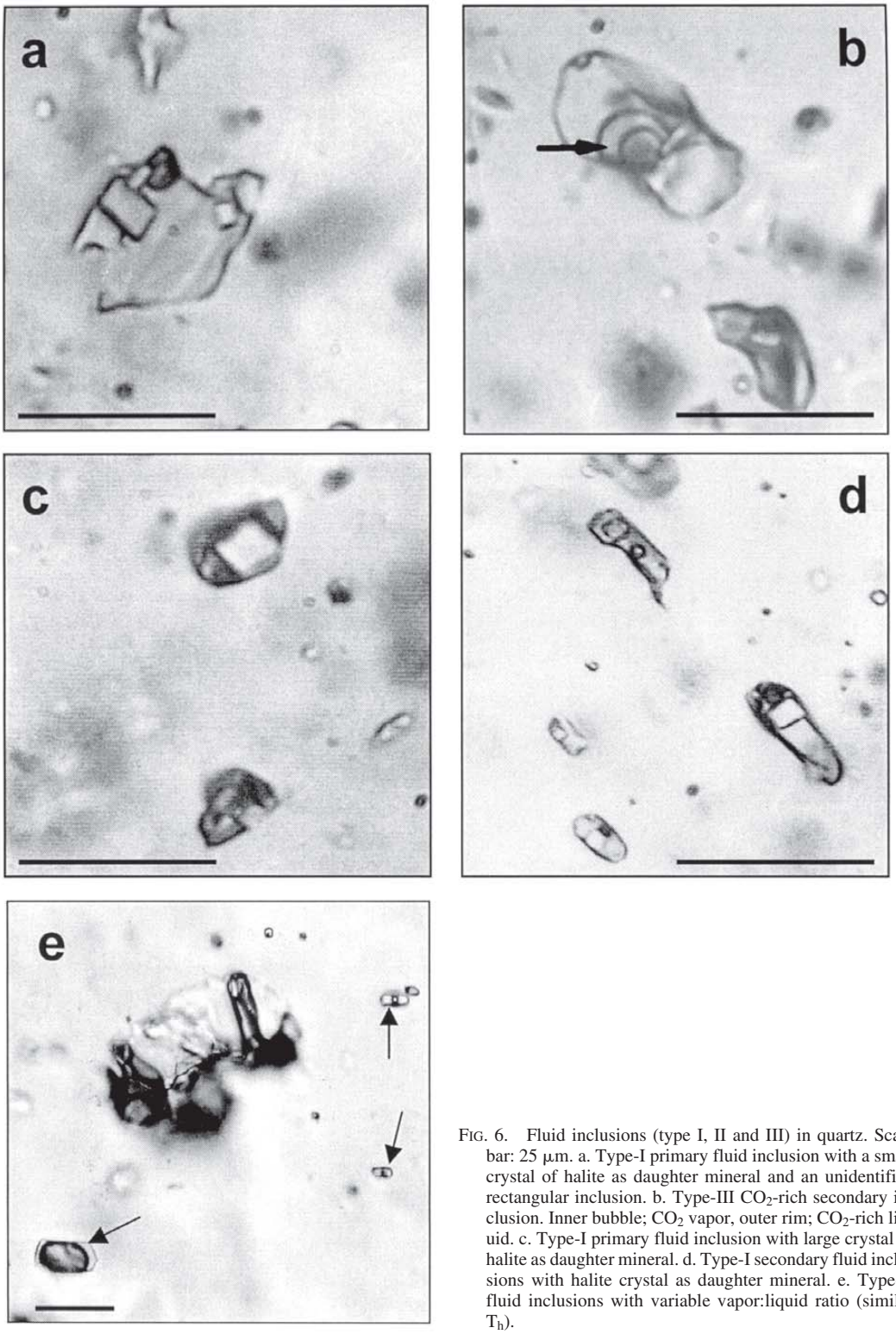

FIG. 6. Fluid inclusions (type I, II and III) in quartz. Scale bar: 25 μm. a. Type-I primary fluid inclusion with a small crystal of halite as daughter mineral and an unidentified rectangular inclusion. b. Type-III CO_2-rich secondary inclusion. Inner bubble; CO_2 vapor, outer rim; CO_2-rich liquid. c. Type-I primary fluid inclusion with large crystal of halite as daughter mineral. d. Type-I secondary fluid inclusions with halite crystal as daughter mineral. e. Type-II fluid inclusions with variable vapor:liquid ratio (similar T_h).

individual grains of quartz. Approximately two-thirds of the primary fluid inclusions are of type I, and one third are of type II. The type-I fluid inclusions contain one or more solid phases, such as halite and accidental inclusions. Some of the accidental inclusions are long prisms or irregularly shaped large plates with low relief, and some are isotropic grains.

Secondary fluid inclusions occur in linear arrays in individual quartz grains in the veins. They are generally controlled by fractures that terminate within grain boundaries or traverse grain boundaries. Some, but not all, contain halite (Fig. 6d), but most inclusions are predominantly of type II. CO_2-rich inclusions (type III) are also considered to be secondary and occur with some of the type-II secondary inclusions.

Fluid-Inclusion Microthermometry

Type-I fluid inclusions containing halite as a daughter mineral were cooled well below their freezing temperature (–90°C), then slowly heated in order to identify the temperature of first melting, or eutectic temperature of ice (T_e). Because the T_e for these inclusions is between –55 and –65°C, the fluid most likely contains solutes in addition to NaCl, such as $CaCl_2$ (Crawford 1981). However, as hydrohalite could not be positively identified in halite-saturated fluid inclusions, the salinity of the fluid is expressed in terms of NaCl equivalent. The salinity of type-I primary and secondary fluid inclusions was calculated from the temperature of final dissolution of halite (Bakker & Brown 2003), that of type-II inclusions, from the temperature of final melting of hydrohalite (Bakker & Brown 2003), and that of type-III inclusions from the melting temperature of clathrate. The appearance of high-relief aggregates in type-II fluid inclusions at approximately the eutectic suggests that the aggregates are probably hydrohalite. Thus, salinity was calculated from the temperature of final dissolution of hydrohalite. The summary of microthermometric data obtained for fluid inclusions of types I, II and III in individual samples is shown in Table 2.

TABLE 2. SUMMARY OF MICROTHERMOMETRIC DATA FOR FLUID INCLUSIONS FROM QUARTZ VEINS, COBALT HILL PROSPECT, ONTARIO

Sample	Type	No.	T_e (range)	T_m (HH)	Salinity ± sd	$T_{h(V)}$ ± sd	$T_{h(salt)}$ ± sd	T_m (CO_2)	T_m (clath)
Primary inclusions									
CH-7C	I	21	(-) 52-61		34.1 ± 2.1	143.±33.2	264±19		
range						120-250	220-350		
CH-7C	II	4				210±21.3			
range						179-230			
CH-7B	I	10	(-) 59-62		35.4±4.3	174±91	257±56		
range						114-384	215-390		
CH-4	I	33	(-) 59-66		34.7±2.8	165±45.1	225±19		
range						109-200	182-240		
CH-7	I	3	(-) 48-55		39.8±0.3	180±13.4	321±3.0		
range						161-189	161-330		
CH-7	II	5		-2.1	25.9	307±37.5			
range						232-330			
Secondary inclusions									
CH--7	II	3	-22	-1.7	26.0	140±3.4			
range						137-145			
CH-7C	II	8	-22	-0.53	26.2	204±17			
range						135-230			
CH-4	I	5			31.1±2.6	109±11	211±18.5		
range						98-120	180-225		
CH-7C	III	5			18.5±0.1	137±3.1		-56.6	-3.5
range						132-141			

No.: number of fluid inclusions measured, T_e: eutectic temperature, T_m (HH): melting of hydrohalite, salinity: equiv. wt% NaCl, $T_{h(V)}$: homogenization temperature of vapor to liquid, $T_{h(salt)}$: dissolution temperature of halite. Salinity is calculated with the program of Bakker & Brown (2003). T_m (CO_2): melting temperature of CO_2, T_m (clath): melting temperature of clathrate.

Primary aqueous fluid inclusions

Several populations of fluid inclusion were identified in the vein quartz. This is apparent in Figure 7, which shows a relatively wide range in the salinity of primary fluid inclusions (25 to 46 equiv. wt% NaCl). Three distinct groups of fluid inclusions are apparent; type II has a narrow range of 24–25 equiv. wt% NaCl, whereas the larger group (type I) has two ranges, 31–35 and 38–40 equiv. wt% NaCl.

In all types of fluid inclusions, homogenization occurred to the liquid phase, with the exception of a few type-II inclusions, where liquid homogenized to the vapor phase. In type-I inclusions, the $T_{h\ (V\rightarrow L)}$ ranges from 100 to 275°C, and $T_{h\ (halite)}$ ranges from 175 to 350°C (Fig. 8). In a single fluid inclusion, $T_{h(V\rightarrow L)}$ at 384°C is similar to the $T_{h\ (halite)}$ at 390°C. Thus, the mode of homogenization of halite-bearing fluid inclusions is consistent for all of the fluid inclusions in the vein quartz, as halite dissolution is invariably preceded by the disappearance of the vapor bubble. As shown in Figure 8, $T_{h\ (V\rightarrow L)}$ is lower by 60–110°C than the dissolution temperature of halite in all of the type-I fluid inclusions. In Figure 9, type-I primary inclusions show a wide range of salinity, 31–46 equiv. wt% NaCl, and T_h, 190°–390°, whereas type-II primary inclusions have a narrow range of salinity, 26–27 equiv. wt% NaCl, but a range of 200° to 335°C for T_h.

In type-I primary fluid inclusions, the minimum temperature of trapping is represented by the halite-dissolution temperature $T_{h\ (total)}$, whereas in type-II primary fluid inclusions, the minimum temperature of trapping is represented by $T_{h\ (V\rightarrow L)}$. Thus the minimum temperature of crystallization of the early quartz vein that contains the pyrite with the inclusions of Ni–Cu sulfide and gold was in the range 190°–390°C (Fig. 10).

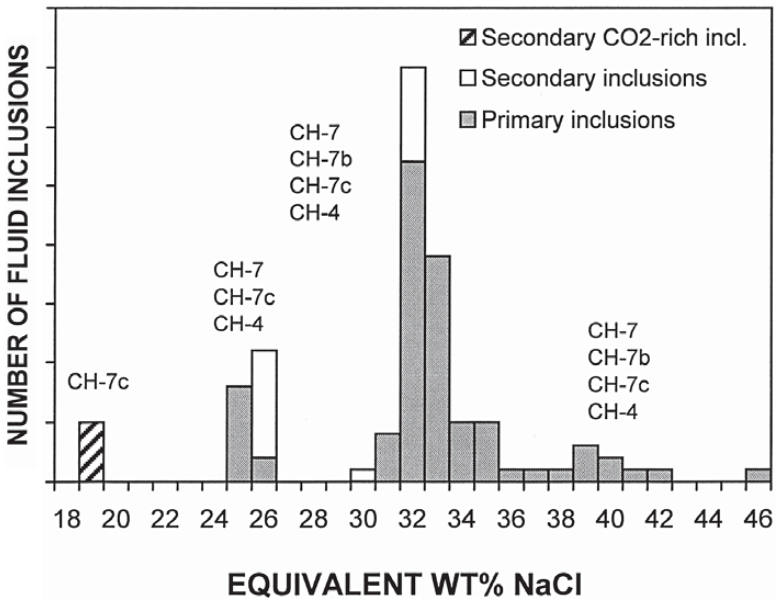

FIG. 7. Salinity histogram of all primary and secondary fluid inclusions.

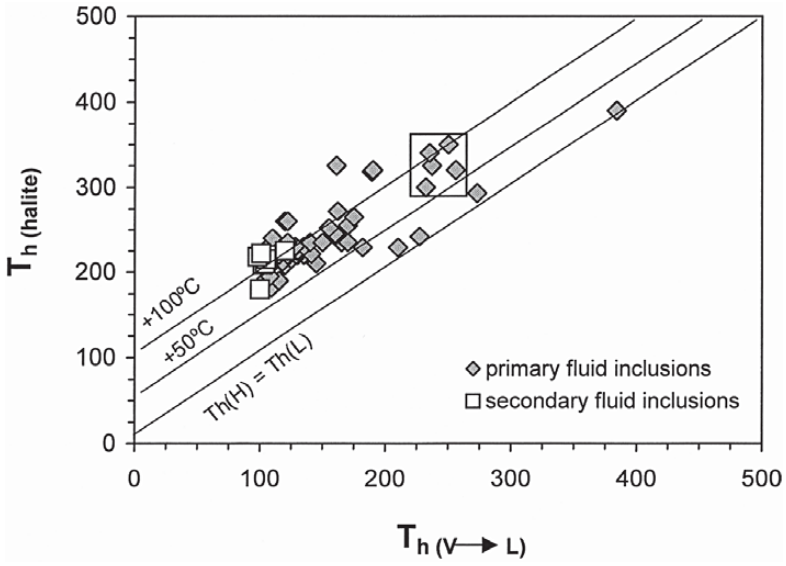

FIG. 8. Plot of homogenization temperature (vapor to liquid) of halite in type-I primary and secondary fluid inclusions. Data points in open square represent fluid-inclusion population used for the pressure–temperature diagram in Figure 14.

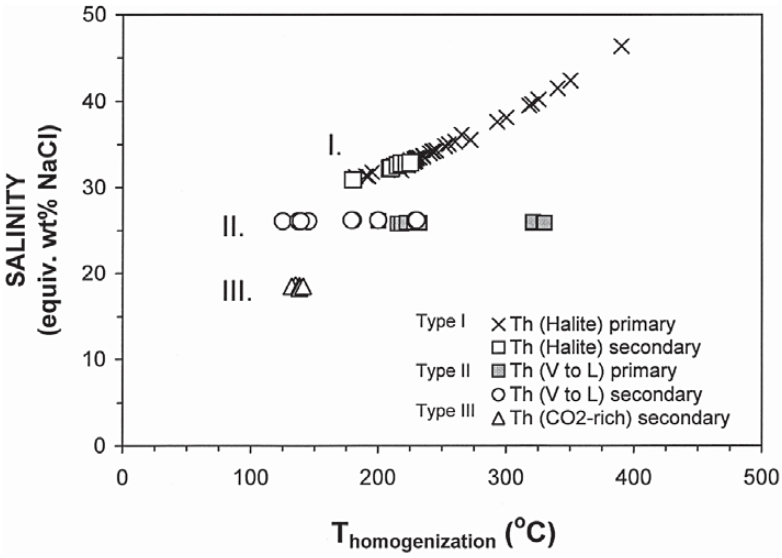

FIG. 9. Plot of salinity *versus* homogenization temperature of primary and secondary fluid inclusions.

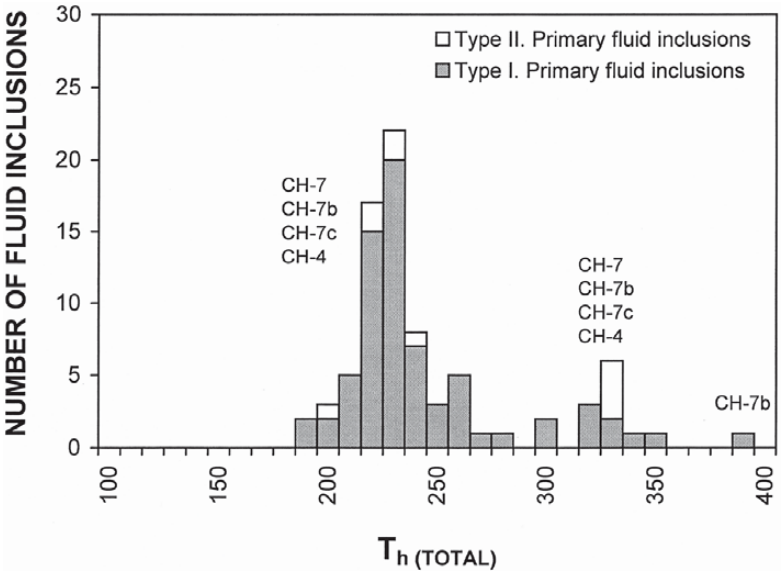

FIG. 10. Homogenization-temperature histogram of type-I and -II primary fluid inclusions.

A limited number of coexisting type-II fluid inclusions show variable vapor-to-liquid ratios in the vein quartz (Fig. 6e), and their comparable T_h (272°–285°C) suggests that boiling probably occurred during the crystallization of the vein. In this case, T_h equals the trapping temperature.

Secondary aqueous fluid inclusions

Three types of secondary fluid inclusions were identified; type I, II and III, having a salinity range of 19 to 32 equiv. wt% NaCl (Fig. 7). Many of the secondary fluid inclusions are free of daughter minerals, but those that contain halite generally have salinities comparable to some of the primary fluid inclusions. In some small two-phase fluid inclusions, the morphology of the fine-grained aggregates of the solid phase during heating, and the sluggish final dissolution of the solids between –0.1 and –2.5°C, suggest that the solid is probably not ice, but hydrohalite (Bodnar 2003). Thus, the salinity was calculated from the temperature of final dissolution of hydrohalite. As shown on Figure 9, the trend of T_h *versus* salinity of type-I primary and secondary fluid inclusions is comparable, although the ranges in salinity (30–32 equiv. wt% NaCl) and T_h (175°–230°C) in the type-I secondary inclusions are narrower than in the primary inclusions. Type-II secondary inclusions have an average salinity of 26 equiv. wt% NaCl and T_h of 130°–230°C (Fig. 9).

Secondary CO_2-rich fluid inclusions

CO_2-rich fluid inclusions are relatively rare in vein quartz. Their morphology is distinctive, as the liquid H_2O contains a central CO_2-rich vapor bubble that is rimmed by liquid CO_2 (Fig. 6b). Microthermometric measurements were obtained from only five CO_2-rich inclusions, as all others decrepitated during heating. The melting temperature of CO_2 at –56.5 to –56.6°C suggests that other dissolved gases (*e.g.*, CH_4) are not present. The salinity of the fluid was calculated from the temperature of final melting of clathrate (–3.2 to –3.8°C), which gives an average salinity of the fluid of 18.5 equiv. wt% NaCl (Fig. 7). Homogenization of CO_2 took place in the range of 22°–24°C, which corresponds to a density of *ca*. 0.8 g/cm^3. The average T_h of the CO_2-rich fluid inclusions at 135°C is much lower than T_h of the type-I and -II primary fluid inclusions, but comparable to some of the type-II secondary inclusions with which they coexist.

Daughter minerals and accidental inclusions in the fluid inclusions

Fluid inclusions were opened in quartz vein fragments, and the daughter minerals and other (accidental) inclusions were examined under scanning electron microscope (SEM) equipped with an energy-dispersion spectrometer (EDS). Elements present in the individual inclusions were identified (qualitative analysis), and some of the daughter minerals and accidental inclusions are shown on Figures 11a–f. The most common solid inclusion in the cavities is halite, some of which contains Fe, and trace amounts of Sn and Au. Although the Sn and Au peaks are minute in comparison with the large Si peak that represents the host quartz, and the Na and Cl peaks of halite, they are distinct. Another (less common) daughter mineral in the fluid inclusions is Fe chloride (Fig. 11c). Accidental inclusions identified in the cavities are pyrite (Fig. 11d), muscovite (Figs. 11e, f), and Fe carbonate.

Discussion

Fluid-inclusion microthermometry combined with mineralogy suggests that the pyrite-rich quartz veins in the fractured, brecciated, and hydrothermally altered quartzites at Cobalt Hill were generated by saline, metal-bearing fluids. That the crystallization of pyrite was contemporaneous with the emplacement of quartz veins is suggested by the presence of small euhedra of pyrite in fluid-inclusion cavities within vein quartz (Fig. 11d). Pyrite in the veins contains an abundance of small inclusions of Cu–Ni sulfides, coloradoite and gold, suggesting that saline fluids mobilized these metals from an unknown source and precipitated them with pyrite. The type and variety of minute inclusions of sulfide (pentlandite, pyrrhotite, gersdorffite, millerite, chalcopyrite and chalcocite) in a single grain of pyrite suggest that the fluids were in contact with base-metal sulfides at some depth. The abundance of muscovite in fluid-inclusion cavities, which also contain halite and pyrite, suggests that crystallization of the pyrite-rich quartz veins and of the micas was broadly contemporaneous. In addition, the textural relationship between muscovite, chromian muscovite and chlorite also suggests that the crystallization of chlorite and the micas was more or less contemporaneous. Thus, some of the fractures (filled by micas and chlorite) in quartz and pyrite probably developed during the emplacement of the veins. The wide range in T_h and salinity within primary fluid inclusions (Fig. 12), the evidence for phase separation (boiling) in some inclusions, coupled with fracturing and brecciation of the vein quartz, imply fluctuating pressure and temperature of the fluid during the evolution of the veins.

The T_h of the primary fluid inclusions represents the minimum temperature at which the host vein of quartz could have crystallized. However, a pressure correction must be applied to the T_h to obtain the true temperature of crystallization. Pressure can be estimated from measurements obtained on halite-bearing fluid inclusions (Bodnar 1994), as achieved by combining the temperature of T_h(H) with the T_h(L,V) of the same inclusions. Figure 8 demonstrates the homogenization behavior of the three-phase fluid inclusions (liquid – vapor – halite),

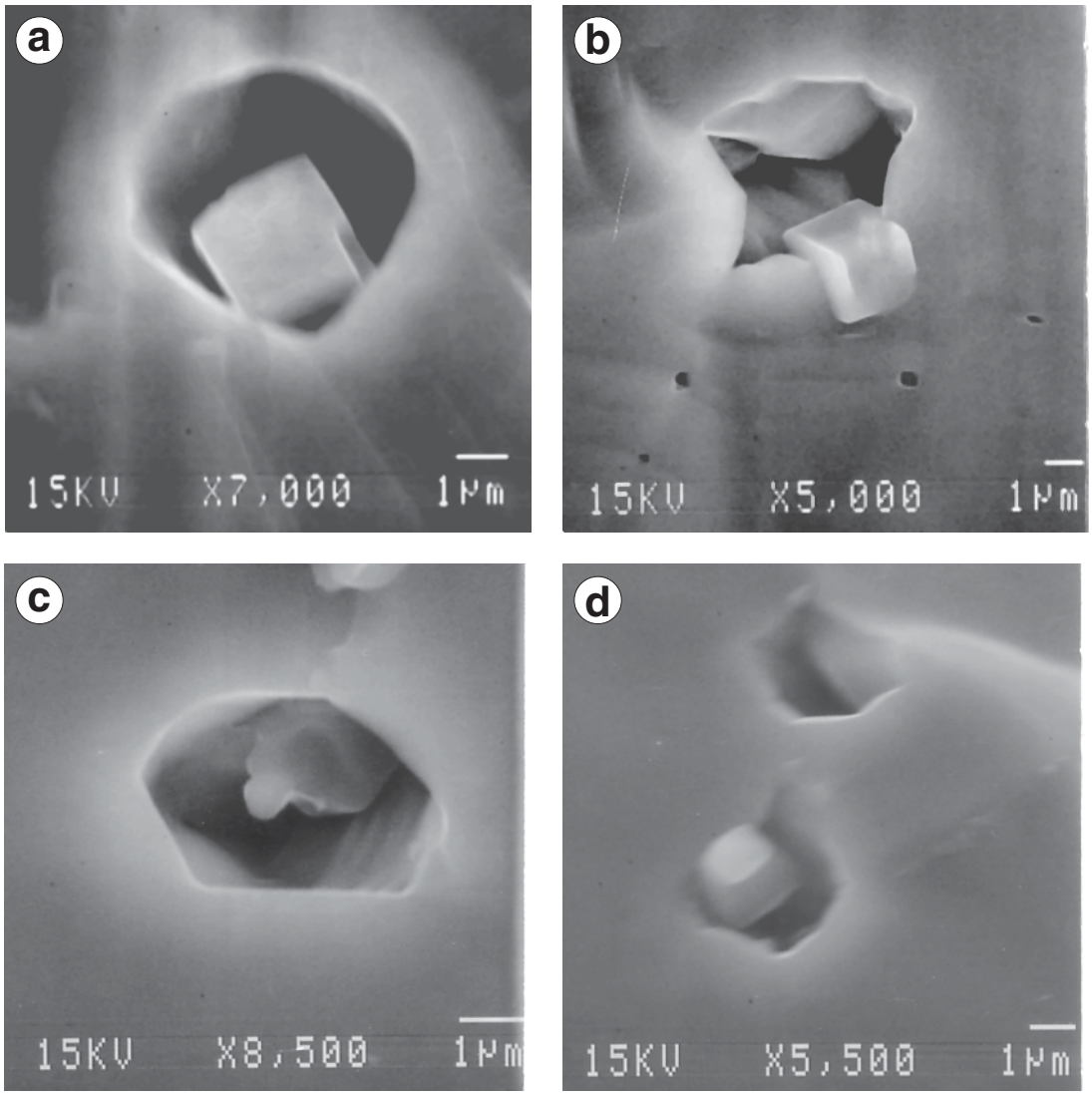

FIG. 11. SEM photographs of daughter minerals and accidental inclusions in open fluid-inclusion cavities. a, b. Cube of halite in inclusion cavity and on inclusion wall. c. Subrounded chloride in inclusion cavity consists of Fe, Na and Cl. d. Pyrite cube consisting of Fe and S in fluid inclusion cavity. e, f. Book of muscovite in fluid-inclusion cavity. g. Halite and muscovite in fluid-inclusion cavity. h. Subrounded halite in fluid-inclusion cavity (with minor Sn and Au).

and Figure 13 is a complementary diagram for fluid of 40 wt% equiv. NaCl, used for estimating P–T conditions for a fluid of appropriate salinity (*i.e.*, 40 wt% equiv. NaCl). Figure 8 shows the trapping of fluids along the $T_h(H) = T_h(L)$ line, and the maximum temperature of halite dissolution for a group of fluid inclusions (at *ca.* 330°C) where ΔT for $T_h(H)$ and $(T_hL,V) = 70$. This information was used in Figure 13 to determine the P–T conditions for the fluid. The pressure, as constrained by the ΔT for $T_h(H)$ and $T_h(L,V)$, was estimated at 1.3 kbar. If the fluid having a T_h of 330°C is projected up the iso-T_h line on Figure 13, one gets a maximum temperature of formation of ≥400°C for the vein quartz that contains the Cu–Ni sulfide inclusions. The 1.3 kbar pressure was also applied to lower-temperature halite-bearing fluid inclusions having a T_h range of 160°–260°C. The pressure-corrected temperature range for these fluids is 220–320°C.

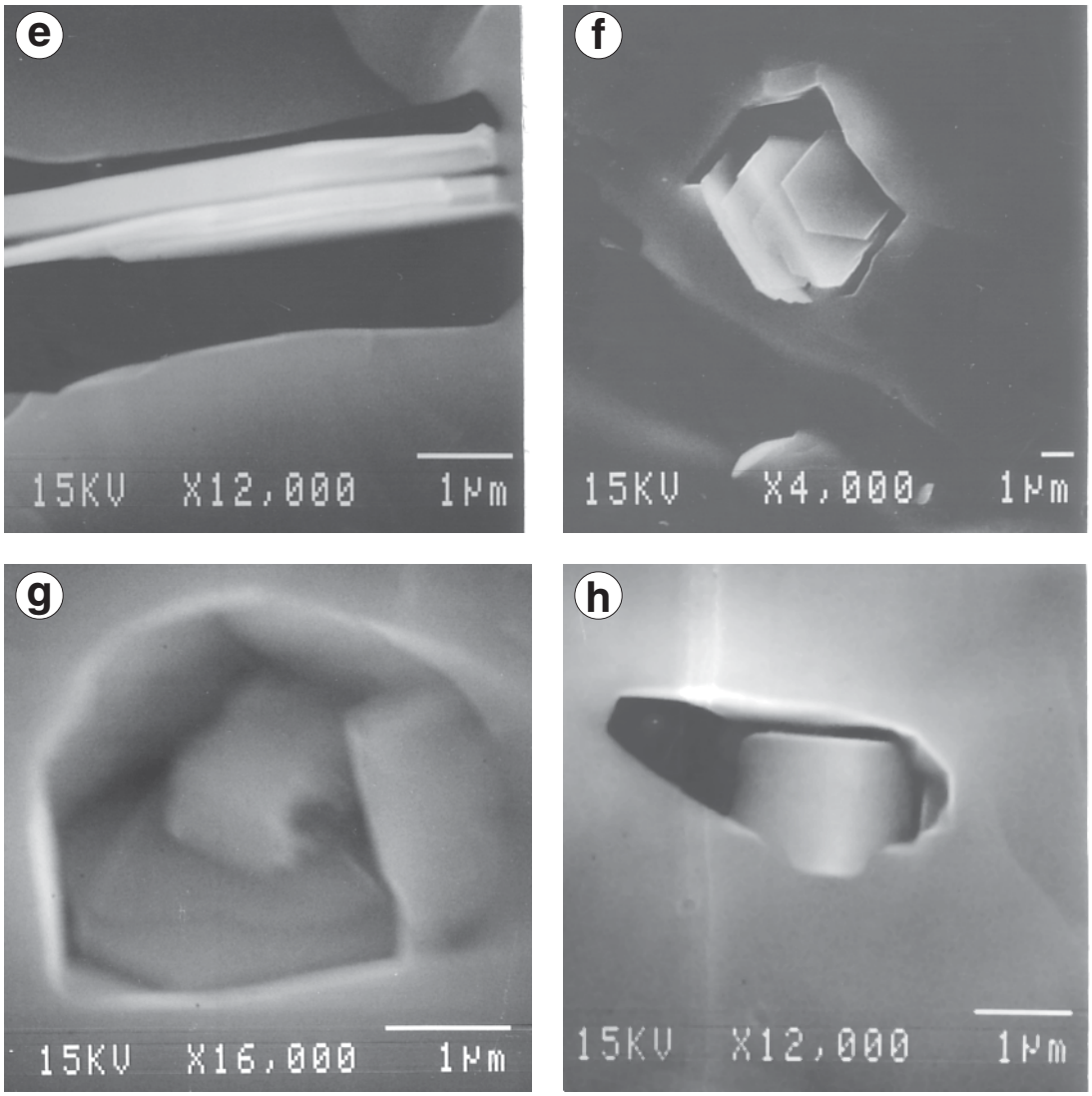

The calculated temperature of chlorite in the fractured vein quartz, 316 ± 25°C (Fig. 13), suggests that the crystallization of chlorite occurred during cooling of the fluids. This lower chlorite-based temperature is consistent with the crystallization of chlorite during fracturing of the vein quartz.

The best estimate of temperature (≥400°C) and salinity (25–46 eq. wt% NaCl) of fluids in primary fluid inclusions of the Cobalt Hill quartz veins is comparable to those reported from various orebodies in the SIC (Farrow & Watkinson 1992, Farrow *et al*. 1994, Li & Naldrett 1993, Molnar *et al.* 1997, 1999). A pressure of 1.1–1.5 kbar was obtained for the North Range granophyre by Molnar *et al.* (2001). Molnar *et al*. (1997, 2001) demonstrated that the vein-type Cu–Ni–PGE deposits of the North Range of the SIC formed by hot, saline, magmatic fluids (400–480°C) that interacted with primary magmatic ores, remobilizing and redepositing the metals in permeable brecciated zones, whereas the vein-type ores of the South Range deposits formed in the temperature range of 180°–350°C. The fluid that deposited quartz in veins at 200°–380°C and 130°–230°C at the Lindsley mine, remobilized some of the sulfides and PGE and redeposited them in the fractured and brecciated zones (Molnar *et al.* 1997).

The relationship between CO_2-rich and aqueous fluid inclusions at Cobalt Hill is unclear. Their $T_{h\ (vapor \rightarrow liquid)}$ is clearly much lower than the T_h of the aqueous pri-

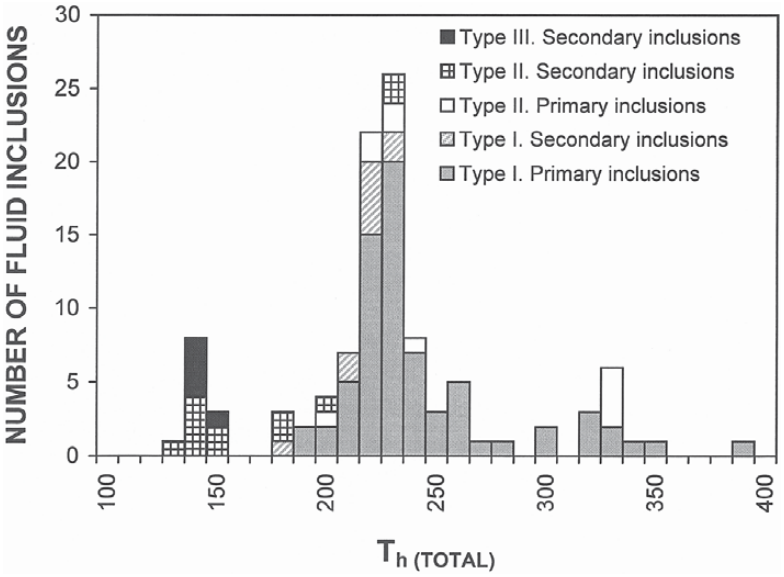

FIG. 12. Temperature of total homogenization of primary and secondary fluid inclusions in vein quartz at Cobalt Hill.

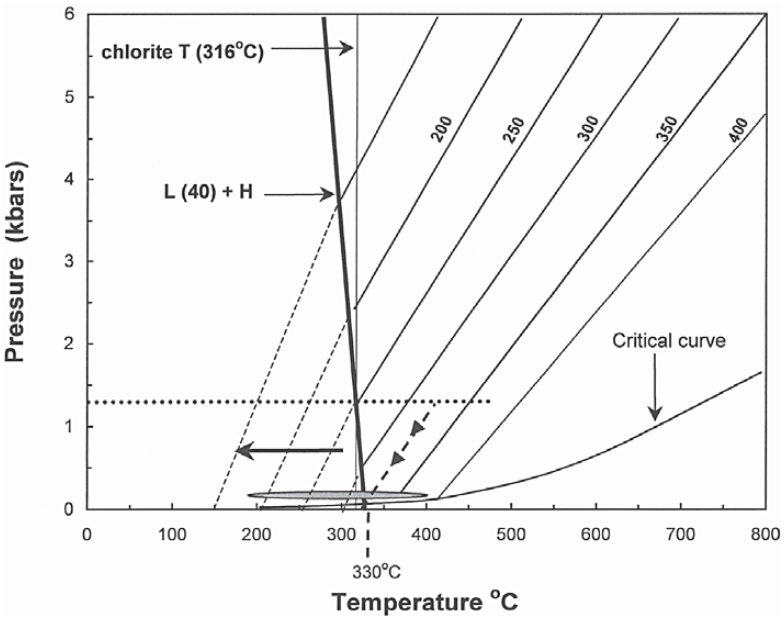

FIG. 13. Pressure – temperature diagram (after Bodnar 1994) used for estimating P–T conditions of formation of the sulfide-bearing quartz veins. The iso-T_h lines are for fluid inclusions containing 40 wt% NaCl, the solid inclined vertical line represents the L(40) + H liquidus, the horizontal dashed line is the estimated pressure on the basis of differences in homogenization between halite and liquid–vapor; $\Delta T(H) - T(L) = 70$, and the horizontal arrow indicates the path of the cooling fluids. The complete range of T_h for the fluid inclusions is shown by the filled horizontal ruler between 160° and 390°C. The thin vertical line represents the calculated (pressure-independent) chlorite-based temperature.

mary fluid inclusions, but comparable to some of the secondary inclusions. Although the present data are insufficient to establish how the CO_2-rich fluids fit into the evolution of the quartz veins, they probably pertain to a separate hydrothermal event that overprinted the mineralized vein quartz.

The paragenetic sequence of various replacement minerals in the Cobalt Hill quartzites suggests that the pyrite-rich quartz veins postdate the 1.85 Ga Sudbury event. The emplacement of pyrite-rich quartz veins into albitized quartzites at Cobalt Hill, and the occurrence of some secondary albite in the quartz veins, suggest that the quartz veins and the albite may have been broadly contemporaneous. The quartz veins were emplaced during a metamorphic event that either slightly postdated the episode of pervasive albitization in the area (at 1.7 Ga; Schandl *et al*. 1994), or it may have been more or less contemporaneous with the waning stages of this episode. The latter is also implied by the abundance of Th-poor hydrothermal monazite (typical of hydrothermal ore deposits; Schandl & Gorton, 2004) in the quartz veins, having similar composition and texture to Th-poor hydrothermal monazite-(Ce) that defined the 1.7 Ga age of sodium metasomatism at the Scadding gold mine in Scadding Township.

As the suite of small base-metal inclusions in pyrite in the quartz veins at Cobalt Hill is comparable to Sudbury-type sulfides, it is not unreasonable to suggest that the base metals were derived by hot saline fluids from magmatic sulfides at some depth. Metals were mobilized from the source by the hot brines that also crystallized the quartz veins. Thus, Cobalt Hill and vicinity have an excellent exploration potential for Sudbury-type mineralization.

The significance of chromian muscovite in the quartzite and quartz veins

In mafic and ultramafic rocks, the source of Cr is pyroxene and chromian spinel. Although chromian spinel is stable under most metamorphic conditions, the replacement of pyroxene by amphibole during metamorphism will liberate a significant amount of Cr that can partition into metamorphic muscovite. Because the amount of Cr in pyroxene is generally proportional to the concentration of Cr in the rock, the amount of Cr released from ultramafic rocks will be significantly more than from mafic rocks. Exceptions are Cr-rich mafic rocks, such as cumulates.

The ubiquitous presence of chromian muscovite over a 180-m section of the Lorrain quartzites in DDH92–1 at Cobalt Hill suggests that Cr was added to the sedimentary rocks and veins from a nearby source. The presence of up to 5–10% chromian muscovite in the veins and sedimentary rocks implies the presence of a Cr-rich igneous body at a depth. This prediction is based on the premise that Cr is one of the most immobile elements in the periodic table; thus, it will not move far from its source once liberated during metamorphism. Such a model was entertained by the author at several well-known gold deposits hosted by pervasively altered ultramafic rocks (*cf.* Dome, Kerr Addison and Aquarius mines in Ontario, and the Cassiar gold mine in British Columbia), where chromian muscovite occurs on the selvages of gold-bearing quartz veins within the ultramafic host. Limited mobility of Cr has been demonstrated at the Kidd Creek VMS deposit in Timmins, Ontario by Schandl (1989) and Schandl & Wicks (1993), where pervasively altered ultramafic rocks consisting of magnesite, quartz and chromian muscovite are in contact with altered rhyolite. Whereas chromian muscovite predominates over white mica in the rhyolite at the ultramafic contact, it gradually decreases in abundance, and finally disappears from the rhyolite at *ca*. 5 m distance from the contact with the ultramafic rock. This finding is consistent with the limited mobility of Cr.

The source of Cr in the Cobalt Hill muscovite is enigmatic, as the only outcropping mafic intrusion, a Nipissing gabbro, is located *ca.* 1 km northwest of Cobalt Hill. Because the Nipissing gabbro suite generally contains only 150–350 ppm Cr (Lightfoot & Naldrett 1996), it would be an unlikely source of Cr. A mafic or ultramafic intrusion that could supply sufficient Cr to account for the presence of chromian muscovite throughout the 180 m thickness of the Lorrain quartzites and quartz veins must be a Cr-rich body that either immediately underlies Cobalt Hill, or is the lateral extension of a buried body adjacent to Cobalt Hill. At present, the only known Cr-rich rocks are the East Bull Lake Intrusive Suite (EBLI) (Easton 1998) and the melanorites and the igneous-textured sublayer of the SIC (Lightfoot *et al.* 1997), which occur 20–25 km south and west of Cobalt Hill. In theory, both the EBLI and SIC could provide sufficient Cr to form the Cobalt Hill chromian muscovite, but their distance from Cobalt Hill makes them unlikely candidates for the source. Nevertheless, the presence of a variety of Ni–Cu sulfide inclusions in pyrite and the relative abundance of chromian muscovite in pyrite-rich quartz veins at Cobalt Hill imply the presence of Cr-rich igneous rocks at depth that have comparable chemical composition and sulfide mineralogy to the SIC and, possibly, the EBLI.

Conclusions

1. Coarse-grained pyrite with minute inclusions of pentlandite, millerite, gersdorffite, pyrrhotite, chalcopyrite, chalcocite, coloradoite and gold was deposited from saline fluids in quartz veins at the Cobalt Hill prospect, 20 km northeast of the SIC. The salinity of the fluid was in the range of 25–46 equiv. wt% NaCl, the temperature of formation of the quartz veins was ≥400°C, and the pressure was approximately 1.3 kbar. The salinity of the Cobalt Hill fluids, and the entrapment temperature and pressure for the pyrite-rich quartz veins are

comparable to P–T conditions associated with some of the vein-type ores of the Sudbury Ni–Cu–PGE deposit (*cf.* Molnar *et al*. 1997, 1999, 2001).

2. The ubiquitous occurrence of chromian muscovite in quartz veins and the host quartzite between 335 and 680 m depth at Cobalt Hill suggests the presence of a Cr-rich mafic or ultramafic intrusion at comparable depths. The variety of Ni–Cu sulfides, pyrrhotite, coloradoite and gold inclusions in pyrite suggests that this hypothetical intrusion contains Sudbury-type assemblage of sulfides.

3. The absolute age of the Cobalt Hill quartz veins has not been determined, but the textural relationship among the assemblages of various alteration minerals suggests that the veins postdated the Sudbury event. Mineralization may have been more or less contemporaneous with waning stages of the widespread 1.7 Ga episode of albitization in the area (Schandl *et al*. 1994). This age is considered to be the time of granitic plutonism in the Southern Province, the time of collisional orogeny, and the development of the Killarney magmatic belt (Easton 1991).

4. The metal-transporting saline fluids that crystallized the pyrite-rich quartz veins at Cobalt Hill were probably heated Canadian Shield brines. The variety of small Sudbury-type assemblage of sulfide inclusions and gold in the pyrite, and the salinity and temperature of fluids at Cobalt Hill, are comparable to the SIC sulfide ores and to the fluids that remobilized and precipitated some of the Sudbury ores. It should be noted that although there are differences in alteration assemblages between the sulfide-bearing quartz veins at Cobalt Hill (muscovite, carbonate, albite, chlorite) and the vein-type deposits of the SIC (epidote, actinolite, biotite, chlorite), these differences are considered to result from differences in wallrock mineralogy and composition. The present findings suggests that Cobalt Hill and its surrounding area provides an excellent target for exploration for base-metal sulfides and, possibly, gold.

Acknowledgements

The author thanks Mr. Murdo McLeod, President of Flag Resources Ltd., for his permission to publish the fluid-inclusion and electron-microprobe data obtained on the Cobalt Hill samples. Many thanks to Dr. Colin Bray and Mr. Jake Hanley of the Department of Geology, University of Toronto for the SEM photographs and (qualitative) analyses of daughter minerals in the fluid inclusions. I am also grateful to Professor Mike Gorton for his help with the electron microprobe. Very special thanks to the editor, Bob Martin, and to the much-appreciated constructive criticism and helpful suggestions of the two reviewers, Dan Kontak and Frank Molnar. The manuscript has greatly benefitted from comments by the editor and the reviewers.

References

Allen, J. (2003). Compilation map in Wanapitei Report to Flag Resources (Brooksbank Management Services). Plate 3-2.

Bakker, R.J. & Brown, P.E. (2003): Computer modelling in fluid inclusion research. *In* Fluid Inclusions. Analysis and Interpretation (I. Samson, A. Anderson & D. Marshall, eds.). *Mineral. Assoc. Can., Short Course Notes* **32**, 175-212.

Bodnar, R.J. (1994): Synthetic fluid inclusions. XII. The system H_2O–NaCl. Experimental determination of the halite liquidus and isochores for a 40 wt% NaCl solution. *Geochim. Cosmochim. Acta* **58**, 1053-1063.

_____ (2003): Introduction to aqueous electrolyte fluid inclusions. *In* Fluid Inclusions. Analysis and Interpretation (I. Samson, A. Anderson & D. Marshall, eds.). *Mineral. Assoc. Can., Short Course Notes* **32**, 81-100.

Cathelineau, M. & Nieva, D. (1985): A chlorite solid-solution geothermometer. The Los Azufres (Mexico) geothermal system. *Contrib. Mineral. Petrol.* **91**, 235-244.

Compston, D.M. & Matthai, S.K. (1994): U–Pb age constraints on early Proterozoic gold deposits, Pine Creek Inlier, northern Australia, by hydrothermal zircon, xenotime, and monazite. *U.S. Geol. Surv., Circ.* **1107**.

Craig, J.R. & Scott, S.D. (1982): Sulfide phase equilibria. *In* Sulfide Mineralogy (P.H. Ribbe, ed.). *Rev. Mineral.* **1**, CS-1–CS-110.

Crawford, M.L. (1981): Phase equilibria in aqueous fluid inclusions. *In* Short Course in Fluid Inclusions: Application to Petrology. (E.D. Ghent, L.S. Hollister & M.L. Crawford, eds.). *Mineral. Assoc. Can., Short Course Handbook* **6**, 75-100.

Dressler, B.O. (1982): Geology of the Wanapitei Lake area, District of Sudbury. *Ont. Geol. Surv., Rep.* **213**.

Easton, R.M. (1991): The Grenville Province and the Proterozoic history of the central and southern Ontario. *In* Geology of Ontario (P.C. Thurston, H.R. Williams, R.H. Sutcliffe & G.M. Stott, eds.). *Ont. Geol. Surv., Spec. Vol.* **4**, 715-904.

_____ (1998): New observations related to the mineral potential of the Southern Province and the Grenville Front Tectonic Zone east of Sudbury. *Ont. Geol. Surv., Open File Rep.* **5976**.

_____ (2000): Metamorphism of the Canadian Shield, Ontario, Canada. II. Proterozoic metamorphic history. *Can. Mineral.* **38**, 319-344.

Farrow, C.E.G. & Watkinson, D.H. (1992): Alteration and the role of fluids in Ni, Cu, and platinum-group-element deposition, Sudbury Igneous Complex contact, Onaping–Levack area, Ontario. *Mineral. Petrol.* **46**, 67-83.

_____, _____ & JONES, P.C. (1994): Fluid inclusions in sulfides from North and South Range Cu–Ni–PGE deposits, Sudbury structure, Ontario. *Econ. Geol.* **89**, 647-655.

FRAPE, S.K. & FRITZ, P. (1987): Geochemical trends from groundwaters from the Canadian Shield. *In* Saline Waters and Gases in Crystalline Rocks (P. Fritz & S.K. Frape, eds.). *Geol. Assoc. Can., Spec. Pap.* **33**, 19-38.

FRITZ, P. & FRAPE, S.K. (1982): Saline groundwaters in the Canadian Shield – a first overview. *Chem. Geol.* **36**, 179-190.

_____, _____ & MILES, M. (1987): Methane in the crystalline rocks of the Canadian Shield. *In* Saline Waters and Gases in Crystalline Rocks (P. Fritz & S.K. Frape, eds.). *Geol. Assoc. Can., Spec. Pap.* **33**, 211-223.

GATES, B.I. (1991): Sudbury mineral occurrence study. *Ont. Geol. Surv., Open File Rep.* **5771**.

GOAD, R.E. (1991, 1992): Unpublished Company Reports to Flag Resources Ltd., Calgary, Alberta.

GUHA, J. & KANWAR, R. (1987): Vug brines-fluid inclusions: a key to the understanding of secondary gold enrichment processes and the evolution of deep brines in the Canadian Shield. *In* Saline Waters and Gases in Crystalline Rocks (P. Fritz & S.K. Frape, eds.). *Geol. Assoc. Can., Spec. Pap.* **33**, 95-101.

INNES, D.G. & COLVINE, A.C. (1979): Metallogenetic development of the eastern part of the Southern Province of Ontario. *In* Summary of Field Work 1979 (V.G. Milne, O.I. White, R.B. Barlow & C.R. Kustra, eds.). *Ont. Geol. Surv., Misc. Pap.* **90**, 184-189.

_____ & _____ (1984): The regional metallogenetic setting of Sudbury. *In* The Geology and Ore Deposits of the Sudbury Structure (E.G. Pye, A.J. Naldrett & P.E. Giblin, eds.). *Ont. Geol. Surv., Spec. Vol.* **1**, 45-56.

KAMINENI, D.C. (1987): Halogen-bearing minerals in plutonic rocks: a possible source of chlorine in saline groundwaters in the Canadian Shield. *In* Saline Waters and Gases in Crystalline Rocks (P. Fritz & S.K. Frape, eds.). *Geol. Assoc. Can., Spec. Pap*. **33**, 69-79.

KELLY, W.C., RYE, R.O. & LIVNAT, A. (1986): Saline minewaters of the Keweenaw Peninsula, northern Michigan: their nature, origin and relations to similar deep waters in Precambrian crystalline rocks of the Canadian Shield. *Am. J. Sci.* **286**, 281-308.

KRANIDIOTIS, P. & MCALEAN, W.H. (1987): Systematics of chlorite alteration at the Phelps Dodge massive sulfide deposit, Matagami, Quebec. *Econ. Geol.* **82**, 1898-1911.

KROGH, T.E., DAVIS, D.W. & CORFU, F. (1984): Precise U–Pb zircon and baddeleyite ages for Sudbury area. *In* The Geology and Ore Deposits of the Sudbury Structure (E.G. Pye, A.J. Naldrett & P.E. Giblin, eds.). *Ont. Geol. Surv., Spec. Vol*. **1**, 431-446.

_____, KAMO, S.L. & BOHOR, B.F. (1996): Shock metamorphosed zircons with correlated U–Pb discordance and melt rocks with concordant protolith ages implicate an impact origin for the Sudbury Structure. *In* Earth Processes: Reading the Isotope Code. *Am. Geophys. Union, Geophys. Monogr*. **95**, 343-353.

KYSER, T.K. & KERRICH, R. (1990): Geochemistry of fluids in tectonically active crustal regions. *In* Fluids in Tectonically Active Regimes of the Continental Crust (B.E. Nesbitt, ed.). *Mineral. Assoc. Can., Short Course Handbook* **18**, 133-230.

LEECH, R.W. & PEARSON, R. (1981): Hydrological research in support of the Canadian Nuclear Fuel Waste Managements program: the Aitikokan, northwest Ontario research area. *Geol. Assoc. Can., Program Abstr.* **6**, A34.

LI, CHUSI & NALDRETT, A.J. (1993): High chlorine alteration minerals and calcium-rich brines in fluid inclusions from the Strathcona Deep Copper zone, Sudbury, Ontario. *Econ. Geol*. **88**, 1780-1796.

LIGHTFOOT, P.C., KEAYS, MORRISON, G.G., R.R., BITE, A. & FARRELL, K.P. (1997): Geologic and geochemical relationships between the contact sublayer, inclusions, and the main mass of the Sudbury Igneous Complex: a case study of the Whistle Mine embayment. *Econ. Geol.* **92**, 647-673.

_____ & NALDRETT, A.J. (1996): Petrology and geochemistry of the Nipissing gabbro: exploration strategies for nickel, copper and platinum group elements in a large igneous province. *Ont. Geol. Surv., Study* **58**.

MACDONALD, A.J. & SPOONER, E.T.C. (1981): Calibration of a LINKAM TH600 programmable heating–cooling stage for microthermometric examination of fluid inclusions. *Econ. Geol.* **76**, 1248-1258.

MARSHALL, D., WATKINSON, D., FARROW, C, MOLNAR, F. & FOUILLAC, A. (1999): Multiple fluid generations in the Sudbury igneous complex: fluid inclusion, Ar, O, H, Rb and Sr evidence. *Chem. Geol.* **154**, 1-19.

MISRA, K.C. & FLEET, M.E. (1973): The chemical composition of synthetic and natural pentlandite assemblages. *Econ. Geol*. **68**, 518-539.

MOLNAR, F., WATKINSON, D.H. & EVEREST, J.O. (1999): Fluid inclusion characteristics of hydrothermal Cu–Ni–PGE veins in granitic and metavolcanic rocks at the contact of the Little Stobie deposit, Sudbury, Ontario. *Chem. Geol*. **154**, 279-301.

_____, _____ & JONES, P.C. (2001): Multiple hydrothermal processes in footwall units of the North Range, Sudbury Igneous Complex, Canada, and implications for the genesis of vein-type Cu–Ni–PGE deposits. *Econ. Geol.* **96**, 1645-1670.

_____, _____, _____ & GATTER, I. (1997): Fluid inclusion evidence for hydrothermal enrichment of magmatic ore at the contact zone of the Ni–Cu–platinum group element 4b deposit, Lindsley mine, Sudbury, Canada. *Econ. Geol*. **92**, 674-685.

NOBLE, S.R. & LIGHTFOOT, P.C. (1992): U–Pb baddeleyite ages of the Kerns and Triangle Mountain intrusions, Nipissing diabase, Ontario. *Can. J. Earth Sci.* **29**, 1424-1429.

PECK, D.C., KEAYS, R.R., JAMES, R.S., CHUBB, P.T. & REEVES, S.J. (2001): Controls on the formation of contact-type platinum-group element mineralization in the East Bull Lake Intrusion. *Econ. Geol.* **96**, 559-581.

ROWELL, W.F. & EDGAR, A.D. (1986): Platinum-group element mineralization in a hydrothermal Cu–Ni sulfide occurrence, Rathbun Lake, northeastern Ontario. *Econ. Geol*. **81**, 1272-1277.

SCHANDL, E.S. (1989): *Talc–Carbonate Alteration of Ultramafic Rocks in the Kidd Volcanic Complex, the Slade Forbes and Munro Asbestos Deposits in the Abitibi Greenstone Belt, Timmins, Ontario*. Ph.D. thesis, Univ. of Toronto, Toronto, Ontario.

_____ (2002): Unpublished Company Report to Flag Resources Ltd., Calgary, Alberta.

_____, DAVIS, D.W., GORTON, M.P., WASTENEYS, H.F. & MARTIN, R.F. (1992): The paragenesis and age of sodium metasomatism in the Espanola – Sudbury – Wanapitei Lake areas. *Ont. Geol. Surv., Misc. Pap.* **159**, 63-79.

_____ & GORTON, M.P. (1991): Postore mobilization of rare earth elements at Kidd Creek and other Archean massive sulfide deposits. *Econ. Geol.* **86**, 1546-1553.

_____ & _____ (2004): A textural and geochemical guide to the identification of hydrothermal monazite: criteria for selection of samples for dating epigenetic hydrothermal ore deposits. *Econ. Geol.* **99**, 1027-1035.

_____, _____ & DAVIS, D.W. (1994): Albitization at 1700 ±2 Ma in the Sudbury–Wanapitei Lake area, Ontario: implications for deep-seated alkalic magmatism in the Superior Province. *Can. J. Earth Sci.* **31**, 597-607.

_____ & WICKS, F.J. (1993): Carbonate and associated alteration of ultramafic and rhyolitic rocks at the Hemingway Property, Kidd Creek volcanic complex, Timmins, Ontario. *Econ. Geol*. **88**, 1615-1635.

Received February 10, 2003, revised manuscript accepted August 11, 2004.

APPENDIX 1.
BRIEF PETROGRAPHIC DESCRIPTION OF SELECTED SAMPLES

CH–1: Quartzite. The rock consists of subrounded quartz grains, lesser relict albite and perthitic K-feldspar, with interstitial aggregates of microcrystalline quartz. Rare white mica occurs in the matrix. Several quartz clasts contain secondary fluid inclusions with daughter minerals (mostly halite). No sulfides, only a few aggregates of rutile.

CH–2A: Granulated quartzite. Quartz clasts are overgrown by chessboard albite. Minor relict albite clasts are also present in the rock, but albitization is evident from partial replacement of granulated earlier silicate (quartz or K-feldspar?) by chessboard albite. Fragmented pyrite occurs within the metasedimentary rock. Pyrite grains contain a few minute inclusions of pyrrhotite and chalcopyrite. Fluid inclusions in quartz do not contain halite as a daughter mineral.

CH–2A–1: Clast-supported quartzite with few orthoclase and albite clasts, interstitial chessboard albite and granulated fine-grained quartz. The rock contains localized segregation of fine-grained apatite, monazite and rutile. The few fragmented grains of pyrite do not contain other sulfide inclusions. Rare secondary fluid inclusions with halite as a daughter mineral are present in some quartz clasts.

CH–2B: Quartzite with some relict albite clasts and a fragmented quartz vein. The rock is albitized, and the very fine-grained interstitial matrix consists of quartz and secondary albite. Some quartz clasts are rimmed by fine-grained chessboard albite, and some seem to be partly replaced by albite. A few grains of pyrite present in the rock are fragmented and granulated. With the exception of a few relict grains, most albite (*ca.* 10 vol.%) is replacement chessboard albite. Secondary fluid inclusions are aqueous and do not contain halite as a daughter mineral.

CH–3A: Fragmented, granulated arkosic quartzite. Chessboard albite forms a rim on some quartz clasts. The matrix is mostly microcrystalline cherty quartz, and the clasts are subrounded quartz grains, angular fragments of earlier quartz vein and relict albite fragments. Inclusion-free fragmented and granulated pyrite appears to be part of the metasedimentary rock. Quartz veinlets cross-cut the rock. A few veinlets of muscovite occur in fractures. Secondary fluid inclusions contain halite as a daughter mineral in quartz clasts.

CH–3B: Fractured arkosic quartzite cut by quartz vein. The quartz vein contains inclusions of albitized clasts. Fracture-filling fine-grained albite veinlets cross-cut the quartz vein. Fine-grained epidote, monazite and zircon aggregates are disseminated throughout the rock. Fractured and fragmented poikiloblasts of pyrite are rimmed by minor white mica and pyrite. Primary fluid inclusions in the fragmented quartz vein are rare, and they are generally free of daughter minerals. Some secondary fluid inclusions contain inclusions of halite.

CH–3C: Sheared, granulated quartzite consists of quartz and a few albite clasts. Some quartz grains are stretched; they are elongate, sheared clasts with mortar-textured matrix. The few grains of fragmented pyrite that occur with fragmented quartz do not contain sulfide inclusions. Fluid inclusions in quartz are secondary and are generally free of daughter minerals.

CH–4A: Fractured quartz vein contains stringers of contorted muscovite and chromian white mica (Table 1) that occur in the fractures. Fine-grained muscovite and fine-grained carbonate aggregates occur as inclusions in quartz. Fluid inclusions in quartz contain halite as a daughter mineral. A few inclusions are CO_2-rich.

CH–4B: Clast-supported quartzite with minor albite clasts. Radiating bundles of chlorite are interstitial to quartz clasts. Some fragmentation and annealing of quartz are apparent. A few aggregates of carbonate and rutile are interstitial to quartz. A few quartz clasts contain fluid inclusions with halite as a daughter mineral.

CH–5: Arkosic quartzite with interstitial microcrystalline quartz matrix. Rutile, monazite and zircon are accessory minerals. Rare muscovite and chromian white mica occur in small veinlets. Secondary fluid inclusions are relatively rare in quartz clasts.

CH–6: Clast-supported arkosic quartzite. It consists predominantly of quartz and lesser albite clasts with fine-grained interstitial, granular quartz matrix. Pyrite poikiloblasts do not contain sulfide inclusions, only fine-grained quartz. Fine-grained muscovite on pyrite, rutile, monazite and zircon are the only accessory minerals present. Fluid inclusions are rare in the quartz.

CH–7A: Coarse-grained plumose quartz in quartz vein. Fine-grained carbonate and muscovite veins are interstitial to quartz. Euhedral grains of pyrite are also interstitial to quartz, and they are rimmed by carbonate. Minute grains of hydrothermal monazite are relatively abundant in the vein. There is an abundance of fluid inclusions (secondary?) in the least-strained quartz, some of which contain halite as a daughter mineral.

CH–7B: Massive quartz vein with minor interstitial bundles of radiating muscovite. Muscovite also occurs in veinlets. Most quartz grains are strained, partly granulated and have the appearance of plumose quartz at the grain boundaries. Euhedral pyrite is interstitial to quartz vein and contains segregations of minute inclusions of Ni–Cu sulfides. Some pyrite (and quartz) are fractured and fragmented. Hydrothermal monazite is abundant; it occurs in quartz and also in fractures. The quartz contains an abundance of fluid inclusions, some of which contain halite as a daughter mineral.

CH–7C: Coarse-grained quartz vein; some quartz grains are fragmented, fractured and partly replaced by an intergrowth of white micas and carbonate. Minor chlorite is interstitial to quartz. Some of the quartz in the vein shows evidence of partial recrystallization at grain boundaries (plumose, pressure-shadow-type quartz). Pyrite grains are interstitial to quartz, some are fractured and fragmented, and contain minute Ni–Cu sulfide inclusions and gold with coloradoite (mercury telluride). Hydrothermal monazite is abundant in the vein. Secondary fluid inclusions are abundant in the quartz, and several contain halite as a daughter mineral.